DOCUMENTATION FILE
Tonzi Ranch Document

August 10, 2006

Written and Edited by D. Baldocchi

AmeriFlux Site: Ione, CA

1. TITLE

Measuring and Modeling Carbon, Water Vapor and Energy Exchange over Grassland and Tree/Grass Ecosystems

PROJECT SUMMARY

Western savanna ecosystems are among the most complex ecosystems to be studied by biometeorologists. They are horizontally and vertically heterogeneous, they experience summer water deficits, and they rely on a multiple plant functional approaches to acquire carbon and manage water loss. At present, savanna ecosystems are poorly represented in the AmeriFlux network. Yet, savannas constitute a major ecosystem and are analogs for studying how the carbon metabolism of ecosystems will respond to environmental perturbations.

We are studying the roles of climate and ecosystem structure and functionality on carbon and water fluxes of an oak/grass savanna and a grassland. This study will provide information on how broadleaved, deciduous forests, in AmeriFlux, respond to changes in soil moisture. It will broaden the range of climate variables, canopy structure and functionality that is currently under study by the network.

The eddy covariance method will be used to measure flux densities of CO_2 and water vapor. Portable eddy flux systems will be deployed in the surface layer and understory of the savanna to augment the tower-based flux measurements. Physiological capacity, sap flow and soil-root respiration will be measured to evaluate fluxes associated with constituent compartments. Our objectives are to assess: 1) the relative contributions of vegetation and the soil on CO_2 and water vapor exchange; 2) spatial variability of understory fluxes; 3) the impact of sloping terrain on the interpretation of flux covariances. A biophysical gas exchange model (CANVEG) and a Lagrangian footprint model will be used to synthesize and interpret the data.

2.0) INVESTIGATOR(S)

2.1) Investigator(s) Name And Title.

Dennis Baldocchi, Principal Investigator, Professor of Biometeorology, Department of Environmental Science, Policy and Management, 151 Hilgard Hall University of California, Berkeley, CA 94720, Baldocchi@nature.berkeley.edu; 510-642-2874 (phone); 510-643-5098 (fax)

Collaborators and Technical Assistance:

Biometeorology Lab
- Dr. Siyan Ma, Associate Specialist
- Dr. Jorge Curiel-Yuste, postdoctoral scientist
- Mr. Ted Hehn, Developmental Technician.

Dr. Todd Dawson, IB/ESPM, UC Berkeley
Dr. Kevin Tu, IB, UC Berkeley
Dr. John Battles, ESPM, UC Berkeley
Dr. Bill Frost, AES/UC Davis

Graduate Students:

Jessica Cruz Osuna
Qi Chen
Xingyuan 'Lorraine' Chen
Gretchen Miller
Youngryel Ryu

Undergraduate
Simon Wong

Former Collaborators and Graduate Students:
Dr. Josh Fisher, Oxford
Dr. Liukang Xu, LICOR
Dr. Jianwu Tang, Univ Minnesota
Dr. Lianhong Gu, ORNL
Dr. Nancy Kiang, NASA/GISS
Dr. Francesca Ponti, University of Bologna

Landholders:
Mr. Russell Tonzi
Mr. Fran Vaira

2.2) Contacts (For Data Acquisition and Production Information).

Dennis Baldocchi, Department of Environmental Science, Policy and Management, 151 Hilgard Hall University of California, Berkeley, CA 94720, Baldocchi@nature.berkeley.edu; 510-642-2874 (phone); 510-643-5098 (fax)

2.3) Requested Form of Acknowledgement.

Dennis Baldocchi, Department of Environmental Science, Policy and Management, 137 Mulford Hall University of California, Berkeley, CA 94720, Baldocchi@nature.berkeley.edu; 510-642-2874 (phone); 510-643-5098 (fax)

Scalar and energy flux data (e.g. CO_2, water vapor, sensible heat and solar energy): Co-authorship if there is extensive use of the data to validate models. Acknowledgement if only few data are used to make a supporting point.

Meteorological data: Acknowledgment.

Acknowledgement: Field data obtained and prepared by Dennis Baldocchi and Liukang Xu (until April, 2004) or Siyan Ma (after May, 2004), Department of Environmental Science, Policy and Management, 151 Hilgard Hall University of California, Berkeley, CA 94720, Baldocchi@nature.berkeley.edu; 510-642-2874 (phone); 510-643-5098 (fax)

3. INTRODUCTION

3.1) Objective/Purpose.

The objective of this research is to measure and model air-surface exchange rates of water vapor, sensible heat and CO_2 over a grazed grassland and oak/grass savanna and to study the abiotic and biotic factors that control the fluxes of scalars in this landscape. Scalar flux densities were measured with tower-mounted measurement systems.

The work to be done addresses three overarching objectives. The first objective of the proposed work is:

> *to establish a new AmeriFlux site and measure and model the biotic and abiotic factors that govern carbon, water and energy exchange of a grassland and an grass/oak savanna over the time scales of hours to days and years.*

The second objective of the proposed work is:

> *to study the impact of heterogeneous canopies and sloping terrain on the measurement and modeling of carbon and water fluxes across a gradient of vegetation and soil.*

The third objective of the proposed work relates to flux footprints and the partitioning of fluxes between the vegetative and soil components. We intend to study:

> *a) the temporal and spatial patterns of soil respiration, evaporation, micrometeorology, canopy structure and energy exchange; b) use this information to parameterize a two dimensional and multi-layer footprint model; c) combine information on wind direction, flux footprints and biomass transects to evaluate the flux climatology of the site.*

As we enter the newest stage of work, we will expand our scope to understand how trends and inter-annual variations in climate affect carbon and water exchange between terrestrial ecosystems and the atmosphere on a decadal time scale. We propose a study that will investigate and quantify the dynamics of net carbon dioxide exchange between the biosphere and atmosphere, which are triggered by such critical features as switches, pulses, lags, and acclimation.

We will upscale the fluxes in space and time with remote sensing and regional weather data. Upscaling will be accomplished in the following manner. First, periodic measurements of high resolution spectral reflectance will be made with a spectral radiometer and continuous measurements of vegetation indices (NDVI and PRI) will be made with an LED spectrometer developed in our lab. Second, relationships between vegetation indices and carbon fluxes will be derived from the field observations. And third, we will apply these algorithms to vegetation indices obtained from MODIS and produce ecosystem-scale estimates of carbon assimilation. We will add a new component to our project that will compare long term eddy flux measurements against changes in stand biomass and soil carbon. These will be based on a sequence of LIDAR measurements and biometry field sampling.

RESEARCH HYPOTHESES

Based on the science and objectives we have introduced and discussed, many interesting questions arise that can form the basis of this research project. Key questions we intend to address in relation to measuring and modeling carbon and water fluxes of a grassland and an oak/grass savanana. They relate to the functionality and variability of carbon and water vapor fluxes in time and space.

Questions relating to functionality include:

1) How do year-to-year variations in annual rainfall, due to the presence of *El Niño* or *La Niña*, affect the carbon and water balances of these systems?
2) How do the carbon and water vapor fluxes of an annual grassland differ from a nearby grass/oak savanna over a spectrum of time scales?
3) How does the mixed grass/tree landscape coordinate the use of water for the gain of carbon over the course time?

Along the vertical spatial axis, we intend to ask:

1) How do vertical differences in physiological capacity, plant architecture and the physical environment integrate to the canopy dimension?
2) What are the relative roles of soil and vegetation on mass and energy exchange?

The main hypotheses we intend to ask with regard to horizontal variability include:

1) Can a flux footprint model be used with a one-dimensional biophysical model to assess fluxes of water and carbon across a patchy landscape or must we consider the advection/diffusion equation in two dimensions?
2) How does sloping terrain affect the conventional measurement of eddy fluxes over short vegetation? Does CO_2 leak out of the control volume as air drains out of the system close to the ground?
3) What are the relative contributions of biodiversity (a mix of species and functional types) on land-atmosphere trace gas exchange? Can we assess this flux by integration information on wind direction, the flux footprint, the biomass distribution and how fluxes respond to climate?
4) How do trees modify the microclimate and ecophysiological functioning of nearby grass? Consequently, is it better for grass to grow under a tree, where it experiences less evaporative demand (but less rainfall) or out in the open, nearby?

With a gradient network in northern California and across to Tennessee, we intend to address:

1) How do spatial gradients in rainfall and temperature affect canopy leaf area, structure and functioning and biosphere-atmosphere trace gas exchange?

Critical questions relating to temporal variation include:

1) What are the relative contributions of dominant times scales (year, season, day, hour) that cause variations of canopy water and carbon exchange and how do these scales vary with climate and functional type?
2) How do seasonal changes in plant structure, soil moisture and physiological capacity affect annual net fluxes?

- 3.2) Summary of Variables.

Key measured flux variables solar radiation components (albedo, net radiation, incoming solar (near infrared + visible), quantum (visible)) and latent heat, sensible heat, soil heat and CO2 flux densities above the canopy. Key meteorological and soil variables being measured included wind speed, wind direction, air temperature, relative humidity, soil temperature, CO2 concentration. The micrometeorological measurements are supported with periodic measurements of photosynthetic capacity, stomatal conductance, soil respiration, leaf area index, plant height, carbon isotopes of air, soil and roots and pre-dawn water potential.

- 3.3) Discussion.

We are measuring eddy flux densities of CO_2, water vapor and sensible heat and turbulence statistics above a grazed oak woodland near Ione, CA. The site is flat and among the oak/grass savanna biome of eastern California, at the foot of the Sierra Nevada mountains. The forest stand was horizontally homogeneous throughout the area deemed as the flux footprint, a region extending over several hundred meters.

One eddy flux measurement system was mounted on a 20 m walkup scaffold tower. Another flux system was placed in the understory, 2 m above the ground.

The eddy flux densities are determined by calculating the covariance between vertical velocity and scalar fluctuations (see Baldocchi et al., 1988). Wind velocity and virtual temperature fluctuations were measured with identical three-dimensional sonic anemometers. Our experience has also taught us that it is prudent to employ three-dimensional sonic anemometers in forest meteorology applications. When deploying an anemometer over vegetation it is nearly impossible to physically align the vertical velocity sensor normal to the mean wind streamlines; sensor orientation problems typically arise due to sloping terrain and to the practice of extending a long boom upwind from a tower. By deploying a three-dimensional anemometer, we are able to make numerical coordinate rotations to align the vertical velocity measurement normal to the mean wind streamlines. CO_2 and water vapor fluctuations were measured with an open-path, infrared absorption gas analyzer, developed at by LICOR.

Fast response meteorology data were digitized, processed and stored using a microcomputer-controlled system and in-house software. Digitization of sensor signals is performed with hardware on the sonic anemometer. Sensor data are output at 10 Hz. Spectra and co-spectra computations show that these sampling rates are adequate for measuring fluxes above and below forest canopies (Anderson et al., 1986; Baldocchi and Meyers, 1991; Amiro, 1990a). Mass and energy flux covariances are be stored at half-hour intervals. Instantaneous data was recorded continuously. Scalar fluctuations and flux covariances are computed post experiment using Reynolds averaging over 30 minute periods. We also apply despiking routines, as the new sonic anemometer and open path sensor spike several times per run. Without spike removal, the flux covariances are very noisy

Proper interpretation of experimental results and model evaluation requires detailed ancillary measurements of many environmental variables. Energy balance components that were measured include the net radiation balance, soil heat flux and canopy heat storage

4.0) THEORY OF MEASUREMENTS

4.1 Micrometeorological Measurement Theory.

A client of mass and energy flux information want to know how much material is being transferred across the land/air interface. Due to practical and theoretical circumstances micrometeorologists cannot place their sensors directly at this interface. Instead, they must make measurements several meters above the land surface and rely on the application of theories, which are derived from the conservation equations of mass, momentum and energy to interpret fluxes made several meters above the underlying surface. The equation defining the conservation of mass and energy provides the guiding principles for designing and executing micrometerological experiments over land surfaces. Mathematically, this equation can be derived by considering the mass flow of material in and out of a conceptual cube (u c). By applying Reynolds decomposition to the velocity and scalar variables and then time averaging, this equation is expressed, in tensor notation as:

$$\frac{d\bar{c}}{dt} = \frac{\partial \bar{c}}{\partial t} + \bar{u}_i \frac{\partial \bar{c}}{\partial x_i} + \bar{c} \frac{\partial \bar{u}_i}{\partial x_i} = -\frac{\partial \overline{u_i' c'}}{\partial x_i} + S_B(t, x_i) + S_{ch}(t, x_i) \quad (1$$

The total time rate of change of a scalar (dc/dt) is a function of its local time rate of change plus the advection of material across the lateral. These terms equal the flux divergence and source/sink strengths due to biology (S_b) and chemical reactions (S_{ch}).

The terminology associated with tensor notations suggests the space, x_i and velocity, u_i variables are incremented from 1 to 3. For the space dimension this corresponds to the longitudinal (x), lateral (y) and vertical (z) dimensions. For velocity, this incrementing corresponds with u, v and w velocity vectors, at are aligned in the x, y and z spatial coordinates.

For the simple case of steady state conditions (dc/dt = 0), horizontal homogeniety (no horizontal gradients) and no chemical reactions, this equation reduces to:

$$0 = -\frac{\partial \overline{w' c'}}{\partial z} + S_B(z) \quad (2$$

Integrating this equation with respect to height yields the classic relationship, from micrometeorological theory is generally applied. We obtain a relation that shows that the eddy covariance between vertical velocity and scalar concentration fluctuations (measured at a reference height, h) equals the net flux density of material in and out of the underlying soil and vegetation, or the net ecosystem exchange of CO_2 (N_e).

$$\overline{w' c'(h)} = \overline{w' c'(0)} + \int_0^h S_B(z) dz \quad (3$$

When the thermal stratification of the atmosphere is stable or turbulent mixing is weak, material leaving leaves and the soil may not the reference height h. Under such conditions the storage term becomes non-zero, so it must be added to the eddy covariance measurement if we expect to obtain a measure of material flowing into and out of the soil and vegetation.

$$\overline{w' c'(h)} + \int_0^h \frac{\partial \bar{c}}{\partial t} dt = \overline{w' c'(0)} + \int_0^h S_B(z,t) dz \quad (4$$

While the storage term is small over short crops, it is an important quantity over forests. With respect to CO_2, its value is greatest near sunrise and sunset when there is a transition between respiration and photosynthesis and a break-up of the stable nocturnal boundary layer by the onset of convective turbulence. With respect to the study of pollutants, the interception of a wandering plume can cause the storage term to deviate from zero.

How can we apply the conservation equation to measure fluxes? In the field, we measure fluxes at a given height above the surface, but we want to know the rate CO2 is taken up by the surface below. The vertical flux density of S will remain unchanged with height if the underlying surface is: 1) homogeneous and extends upwind for a considerable distance (this requirement ensures the development of a surface boundary layer); 2) if scalar concentrations are steady with time; and 3) if no chemical reactions are occurring between the surface and the measurement height.

Condition one can be met easily through proper site selection. As a rule of thumb the site should be flat and horizontally homogeneous for a distance between 75 and 100 times the measurement height (Monteith and Unsworth, 1990). Condition two is met often for many scalars. Non-steady conditions are most apt to occur during abrupt transitions between unstable and stable atmospheric thermal stratification, during the passage of a front or from the impaction of a plume from nearby power plants.

As we attempt to apply micrometerological conditions to over long, time periods and over non-ideal conditions, we must rely on a comprehensive form of the conservation of mass equation and design our experiment on the basis of the terms that need to be assess.

4.2 Eddy Covariance Technique.

The eddy covariance method is a direct method for measuring flux densities of scalar compounds. The vertical flux density is proportional to the covariance between vertical wind velocity (w) and scalar concentration fluctuations (c).

A wide range of turbulent eddies contribute to the turbulent transfer of material. Proper implementation of Eq. 1 requires that we sample across this spectrum of eddies. In frequency domain, eddies contributing to turbulent transfer having periods between 0.5 and 2000s typically contribute to mass and energy exchange (Wesely et al. 1989). Hence, wind and chemical instrumentation must be capable of responding to high frequency fluctuations. And computer-controlled data acquisition systems must sample the instrumentation frequently to avoid aliasing and average the signals over a sufficiently long period to capture all the contributions to the transfer.

On applying the covariance relation, it is assumed implicitly that the mean vertical flux density is perpendicular to the streamlines of the mean horizontal wind flow. Consequently, the mean vertical velocity, perpendicular to the streamlines of the mean wind flow, equals zero. In practice, non-zero vertical velocities occur due to instrument mis-alignment, sloping terrain and density fluctuations. These effects must be removed when processing the data, otherwise mean mass flow can introduced a bias error (see Businger, 1986; Baldocchi et al., 1988).

Evaluating the accuracy of the eddy correlation method is complicated. Factors contributing to instrument errors include time response of the sensor, signal to noise ratio, sensor separation distance, height of the measurement, and signal attenuation due to path averaging and sampling through a tube. Natural variability is due to non-steady conditions and surface inhomogeneities. Under ideal conditions

natural variability exceeds about +/-10%, so it is desirable to design a system with an error approaching this metric.

Moore (1986) discusses transfer functions for sensor response time and separation distance. We preformed preliminary calculations of transfer function integrals. Corrections due to sensor time constants and separation are less than a few percent. Hence, we decided not to make transfer function to our flux measurements; our experimental design minimized the need for such corrections since we used an open path infrared gas analyzer and a sonic anemometer. Furthermore, these instruments were placed over a tall rough forest, so small distances in physical displacement have little impact on the measurement of scalar flux densities.

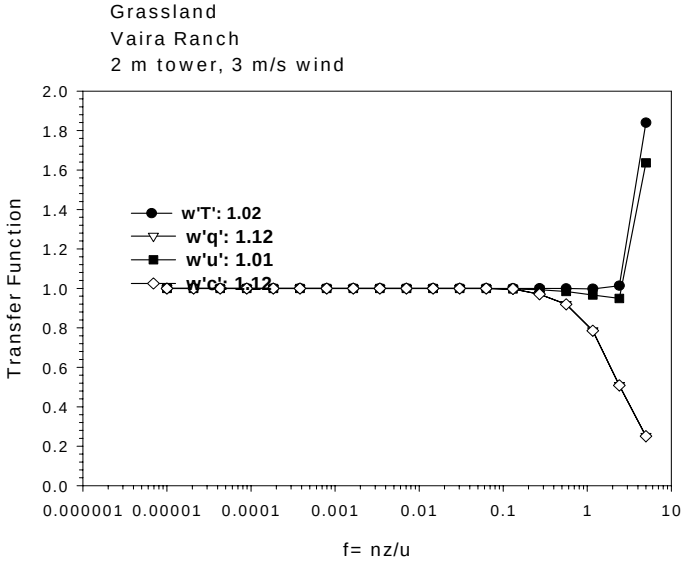

Figure 1 Transfer function of eddy fluxes for the current grassland configureation. Potential errors for moderate winds and stable conditions may reach 10% on the basis of Moore algorithms.

The sensors which are used to measure CO2 fluxes measure CO2 density fluctuations, rather than mixing ratio. Application of the density corrections, attributed to Webb et al. (1980) are applied to our measurements. Corrections to eddy fluxes will be greatest during periods with high sensible heat fluxes, as when the grass is dead and dormant.

The instruments and their employment is design such that most of the power and cospectra are sampled for producing estimates of variances and covariances. Examples are shown next.

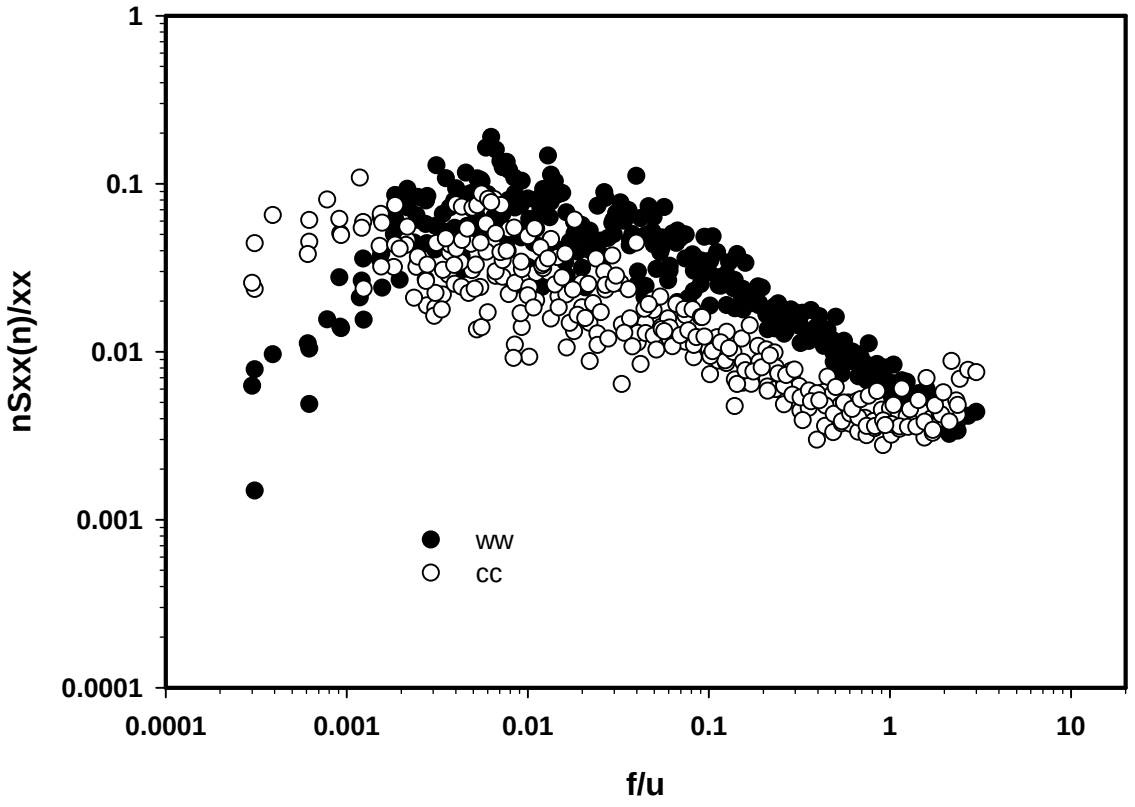

Figure 2 Power spectrum for vertical velocity and CO2 on savanna tower

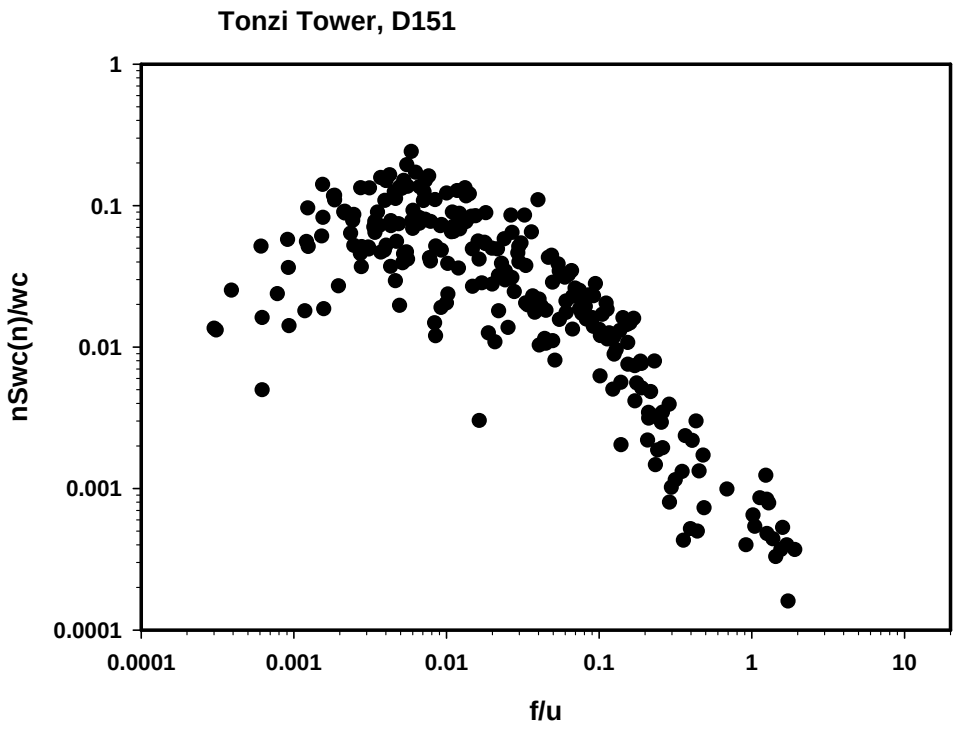

Figure 3 Co2 Co-spectrum over Tonzi ranch

5.0) EQUIPMENT

- 5.1) Instrument Description.

The experiment includes instrument setups for eddy covariance, meteorology and soil physical properties. The eddy Flux system involves measurements of turbulence, vertical, horizontal wind velocities and virtual temperature. The instruments include:

Sonic anemometer: Gill Windmaster Pro,

CO2 and water vapor concentrations: Licor-LI7500

CO2 Gashound, LI-800

Meteorological Variables

PAR incoming: Kipp and Zonen PAR-Lite
PAR reflected: Kipp and Zonen PAR lite
Net radiometer: Kipp and Zonen, NR lite
Pyranometer: Kipp and Zonen
Pressure: Vaisala

Temperature: Vaisala, HMP (sensor U3030042)
Relative humidity: Vaisala, HMP
Rain, Texas Electronics, tipping bucket, TE 5252mm (sensor LX 243734)

Soil variables include

Soil heat flux plates: Huseflux (3)
Soil temperature: UCB probes at 2, 4,8,16 and 32 cm (3)
Soil moisture: Theta probe ML2x, Delta-T Devices (5), 2 at 10 cm, 2 at 20 cm and 1 at surface
Soil CO2: Vaisala at 2, 8 and 16 cm in the open and under a tree

Eddy covariance flux measurements are made using a triple-axis wind master prof sonic anemometer and a Licor 7500 infrared absorption spectrometer. The sonic anemometer measured vertical (w) and horizontal (u,v) wind velocity and virtual air temperature (T). This anemometer model provides digital output at a rate of 10 Hz. The infrared absorption spectrometer measures water vapor and CO_2 density fluctuations. The sensor responds to frequencies up to 10 Hz, has low noise and high sensitivity. The sensor is rugged and experiences little drift over several weeks of continuous operation.

Soil heat flux density is measured by averaging the output of three soil heat flux plates (Huseflux). They are buried 0.01 m below the surface and were randomly placed within a few meters of the flux system. Soil temperature are measured with two multi-level thermocouple probes. Sensors are spaced logarithmically at 0.02, 0.04, 0.08, 0.16 and 0.32 m below the surface.

Photosynthetically active photon flux density, solar radiation and the net radiation balance are measured above the grassland with a quantum sensor (Kipp and Zonen PAR lite), pyranometer (Kipp and Zonen) and a net radiometer (Kipp and Zonen), respectively. A LICOR line sensor (modelxxx) is used to measure light through the grass

Air temperature and relative humidity are measured with appropriate sensors (Vaisala, model HMP-35A).

Static pressure is measured with a Vaisala model PTB101B sensor. It operates on a 600 to 1060 mb range over 2.5 volts.

Ancillary meteorological and soil physics data are acquired and logged on a Campbell CR-23x and CR-10x data loggers. Half-hour averages were stored on a computer, to coincide with the flux measurements.

CO_2 concentration profiles were originally measured with the LICOR 7500. We now have a dedicated profile system using the LI-800 that is zeroed and calibrated 2 times per day. Pressure through the cell is controlled to 1 part per 1000 with a pressure controller. Temperature of the cell is maintained near 50 C and is measured with an independent thermocouple.

A radiation tram system was installed in the forest understory during the spring of 2006. A net radiometer and up and down facing quantum sensor will traverse back and forth along a 30 m transect.

- 5.1.1 Principles of Operation.

Sonic Anemometer:

Three-dimensional orthogonal wind velocities (u,v and w) and virtual temperature (T_V) were measured with a sonic anemometer (Wind Master Pro). The pathlength between transducers was 0.15 m. The sensor software corrected for transducer shadowing effects (see Kaimal et al. 1990). Virtual temperature heat flux was converted to sensible heat flux using algorithms described by Kaimal and Gaynor (1991).

Infrared Absorption Spectrometer:

Water vapor and CO_2 concentrations were measured with an open-path infrared absorption spectrometer.

Soil Heat Flux Transducer:

An encapsulated thermopile yields a voltage output proportional to the temperature difference across the top and bottom surfaces. The device has been calibrated in terms of heat flux through transducer corresponding to the observed temperature difference.

Instrument Measurement Geometry.

The eddy flux measurement system was placed at 2 m above the ground. The Licor 7500 was 0.15 m beside the sensor

Power: solar panels

Siemens SP75 panels in parallel with Morningstar 30 regulator and 6 12 vdc batteries. The forest floor system draw is 2.1 amps. The tower system draws about 4.3 amps.

Six panels run the floor system and the tower systems.

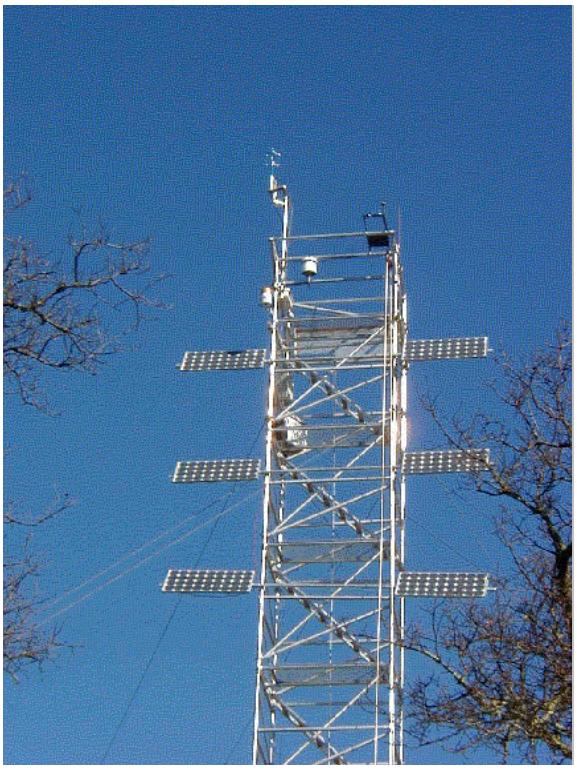

Manufacturer of Instrument.

Gill/Solent Sonic anemometer:
Model: WindMaster Pro

3 wind vectors
Sonic (virtual) temperature
4 channels A/D, 12 bit resolution

Soil heat transducer:

HuseFlux

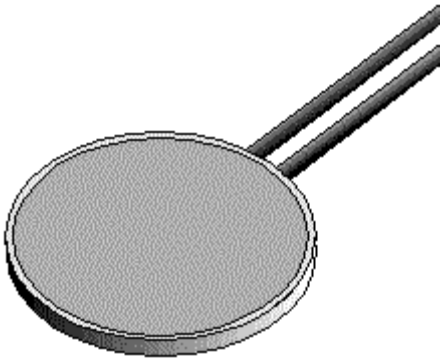

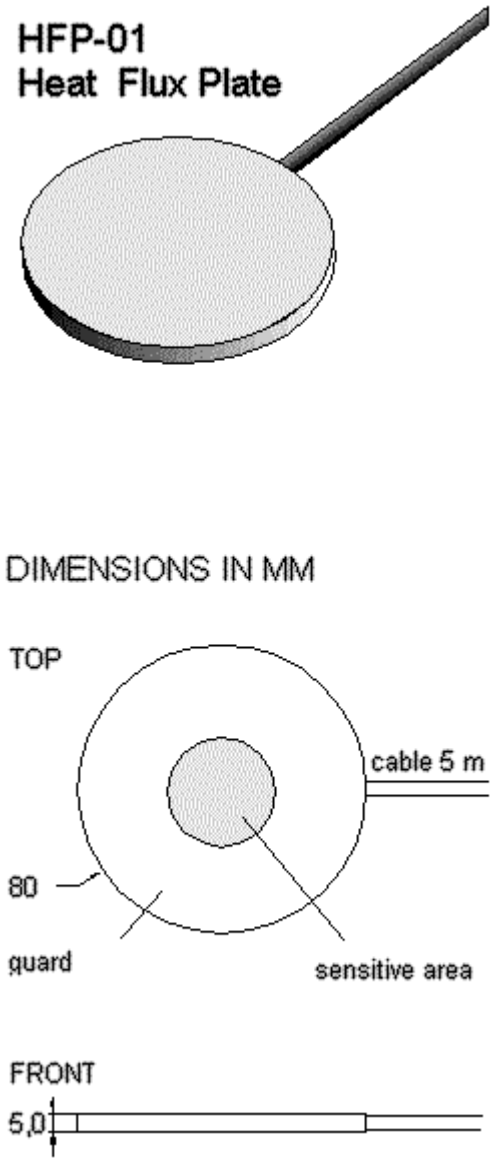

Figure 4

Net Radiometer:

Kipp and Zonen, NR-Lite

Pyranometer and Quantum Sensors

Kipp and Zonen, Pyranometer

Data logging system:

Campbell Scientific
P. O. Box 551,
Logan, UT 84321

CO2/water vapor analyzer

LI 7500

LICOR
4421 Superior St
Lincoln, NE

Temperature and humidity

Vaisala

Pressure Sensor

Static
Vaisala

Physiology

LI 6400

Licor

Soil respiration chamber

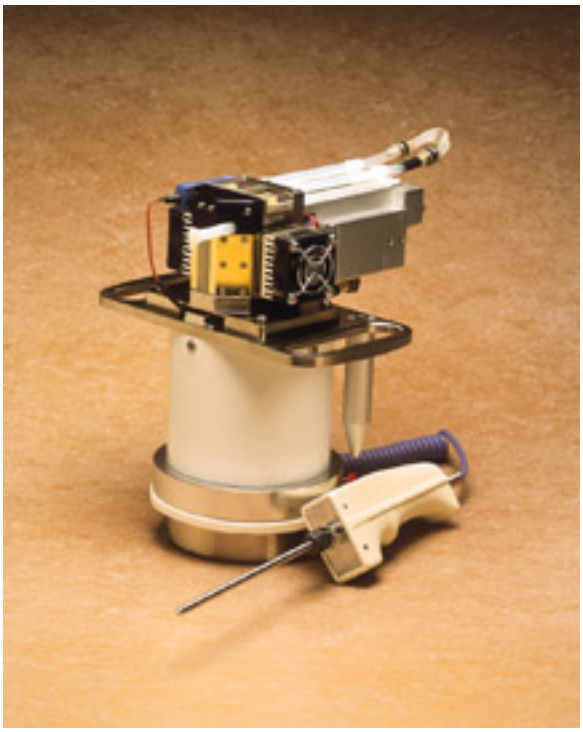

Pressure bomb

Plant water status console

Wind Profile (set up D212, 2003)

Handar, now Vaisala

Wind speed profile system sensor heights:

Level	Height (Meter)
1	10.61
2	11.76
3	13.21
4	15.04
5	16.86

Soil CO2 profiles
Vaisala GMT 220 CARBOCAP sensor

Sensor Location.

We are operating a flux system on a 20 m walk up tower an in the understory on a 2 m tower.

A picture of the site and instrumentation is shown below.

Figure 5 Understory flux system at Tonzi Ranch

Understory flux system

Figure 6 20 m tall walkup tower at Tonzi Ranch, Ione, CA

5.2) Calibration.

Flux and mean concentration CO2 analyzers were calibrated against secondary calibration gases. These gases were referenced to standards prepared by NOAA/CMDL (http://www.cmdl.noaa.gov/ccg/refgases.html)

Trace gas standards used for measuring CO_2 by the Carbon Cycle Group (CCG) of NOAA CMDL are contained in aluminum cylinders purchased from Scott- Marrin, Riverside, California. The cylinders are treated with a proprietary passivation treatment. CCG uses three different size cylinders but most of our standards are contained in 30 liter (internal volume) cylinders. The cylinders are ordered with brass Ceodeux cylinder valves (CGA590) containing all-metal seats and nickel stems. The cylinders are shipped to CMDL with 1380 kPa (200 psig) of dry, ultrapure air. It is important for the cylinders to be dry (and remain dry) during filling and use. Brass cylinder valves rather than stainless steel, are recommended for all trace gas species measured by CCG.

The zero and span of the LICOR infrared gas analyzer, used in the profile system, were measured twice a day.

The water vapor sensor was calibrated against mixed air samples and referenced to data from a chilled mirror dew point hygrometer. Stability of the water vapor calibration was checked in the field by comparing the instrument sensitivity to the output of a Vaisala relative humidity sensor. The relative humidity sensor was new and calibrated by the manufacturer. We also compared the output of the Vaisala relative humidity sensor against a redundant dew point hygrometer. Both sensors yielded identical humidity measurements.

Radiation sensors are calibrated against a set of laboratory standards about once per year.

We periodically send the sonic anemometers, Licor gas analyzers and Vaisala CO2 and T/RH probes back to the manufacturers for lab calibration and maintenance.

- 5.2.1) Specifications. Calibration factors.

Sonic anemometer: supplied by manufacturer. 1.0 m s^{-1}/V with sonic pathlength 0.15 m.

Carbon dioxide:

Water vapor density fluctuations: varies with vapor density

Soil heat transducer:

net radiation:

quantum flux density: 180 μmol m^{-2} s^{-1} mv^{-1}

Pressure: 0.184 mb/mv

- 5.2.1.1) Tolerance. Precision or sensitivity estimates:

Solar and net radiation: 1 W m^{-2}.

Air temperature fluctuations: 0.1 K.

Vertical wind velocity fluctuations: 0.01 m s^{-1}.

Surface radiative temperature; 0.1 K.

Other Calibration Information.

CO2 gases were originally referenced to NIST standards. We have depleted those gases and recently purchased standards from Dr. Pieter Tans, CMDL/NOAA lab.

National Oceanic and Atmospheric Administration
Climate Monitoring and Diagnostics Lab
Carbon Cycle Greenhouse Gases group
R-E-CG1
325 Broadway
Boulder, CO. 80303
E-Mail dkitzis@cmdl.noaa.gov
Phone 303-497-6675
Fax 303-497-6750

http://www.cmdl.noaa.gov/ccgg/refgases/airstandard.html

References

The manometric calibration system is described in more detail in Zhao, C., P.P. Tans and K.W. Thoning, A high precision manometric system for absolute calibrations of CO_2 in dry air. *Journal of Geophysical Research*102(D5):5885-5894 March 20, 1997

6.0) PROCEDURE

6.1) Data Acquisition Methods.

We use a system of daisy changed CR10x and CR23x data loggers, connected via coax cable and Md-9s to log and store the meteorological and soil data. These are tied to a pc which runs the pc208 software. The data are written to disk each 30 min. Once each day the data files are renamed with information on the logger, year and day. For example,

CR23x2 stores data to CR23x2.dat. At midnight this file becomes TZ2_yrday.23x, or file
CR10x4 stored data as CR10x4.dat. At midnight that file becomes TZ4_yrday.10x.

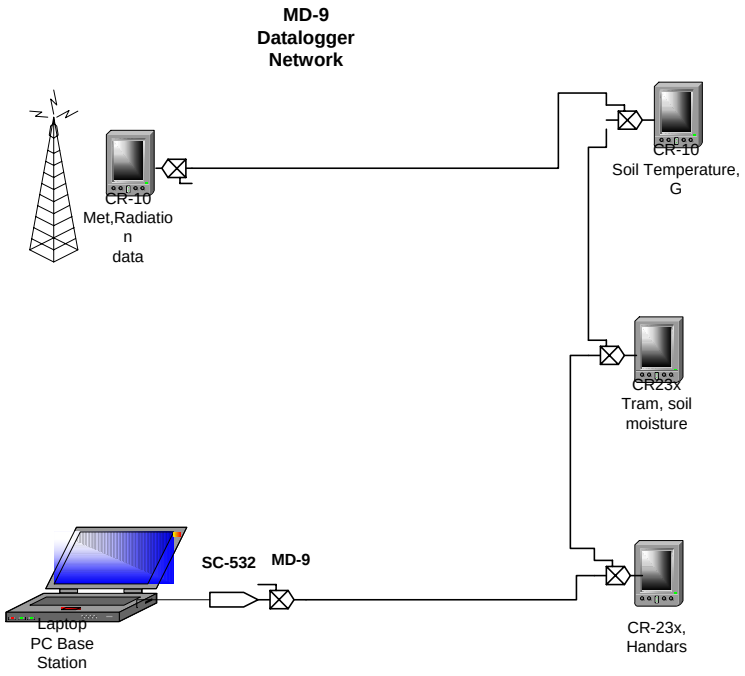

7. SITE CHARACTERISTICS

7.1) Spatial Characteristics.

The field site is located on the near Ione, CA on the property of Mr. Russel Tonzi. The tower is at N 38°25.867', W 120° 57.970'. This converts to Latitude 38.4311 N; longitude 120.966W

Forest floor system is at Lat 38 25.896 N; long 120 57.959 W; alt 177m

Figure 7 View of Tonzi Ranch from Tower

Table 1 Locations of towers and soil moisture probes in UTM coordinates

location	utm_x	utm_y
931AFE	4255607.069	677545.181
402165	4255655.744	677531.328
74B4B	4255665.754	677550.370
402FF3	4255688.471	677510.922
574632	4255691.463	677482.224
7A432E	4255692.321	677498.913
7A3C6E	4255691.970	677470.594
7A3B40	4255691.661	677462.621
7A4AAA	4255690.659	677459.450
Flow Flux System	4255667.396	677524.846
Eddy covariance tower northwest corner	4255589.392	677542.198
Eddy covariance tower southeast corner	4255586.972	677544.014
Grassland soil moisture 1	4253662.283	678916.957
Grassland soil moisture 2	4253659.748	678923.477
Grassland tower system	4253658.868	678914.477

Over the past several years we have collected much leaf, soil and canopy information to characterize the site. We have also collected remote sensing data on the site with images from IKONOS, CASI. MODIS and AVRISS.

With IKONOS we have 1 m resolution PAN chromatic data

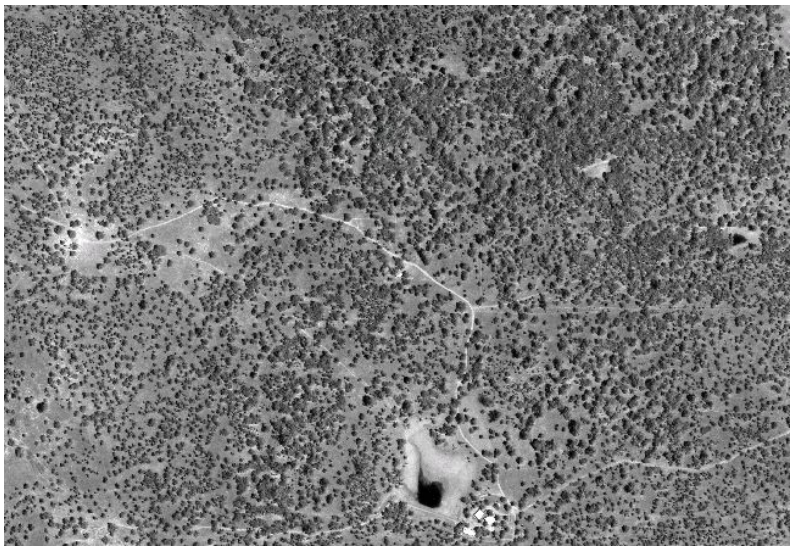

Figure 8 Ikonos Panchromatic image 1 m resolution

We also have 4 m multispectral data. Below is an image of this site in high detail.

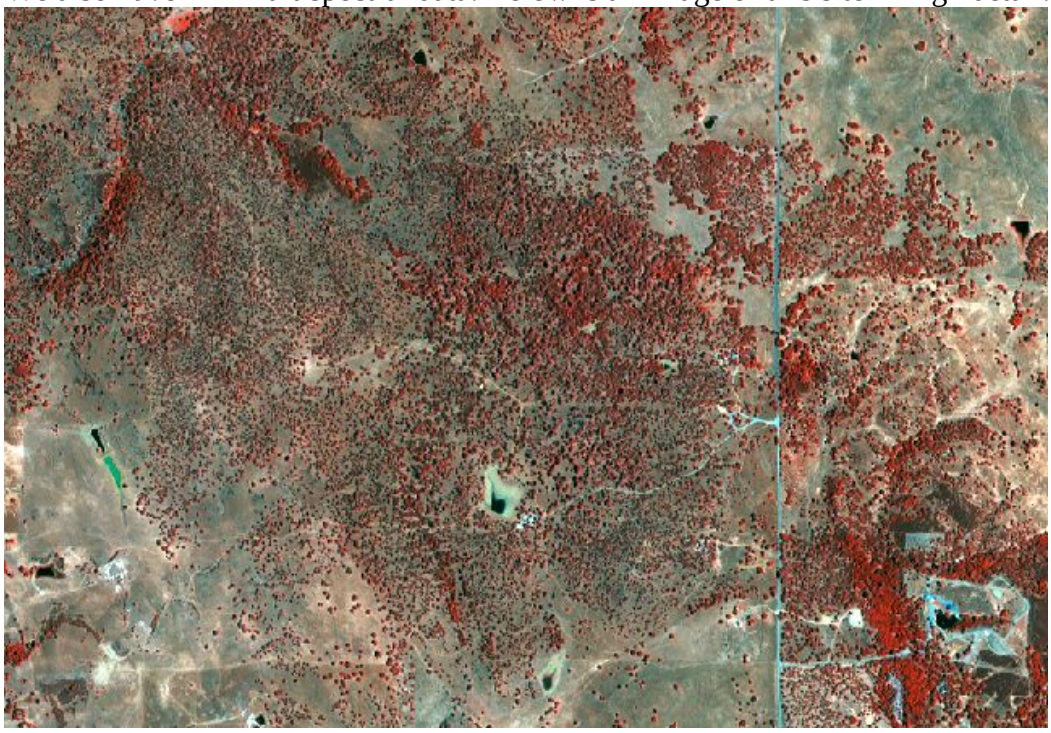

Figure 9 IKONOS Image of Tonzi Ranch Field site, scale of the figure is about 2-3 km across. Pixel resolution of figure is 4 m.

Flux footprint calculations were done at our lab. We find that most of the flux sensed by our eddy covariance instrumentation comes from a region within 300 m of the tower.

The below canopy measurement of net radiation was performed with sensors on a tram that traversed a 30 m transect under the forest. This design was needed to account for high spatial heterogeneity of light near the floor of a forest.

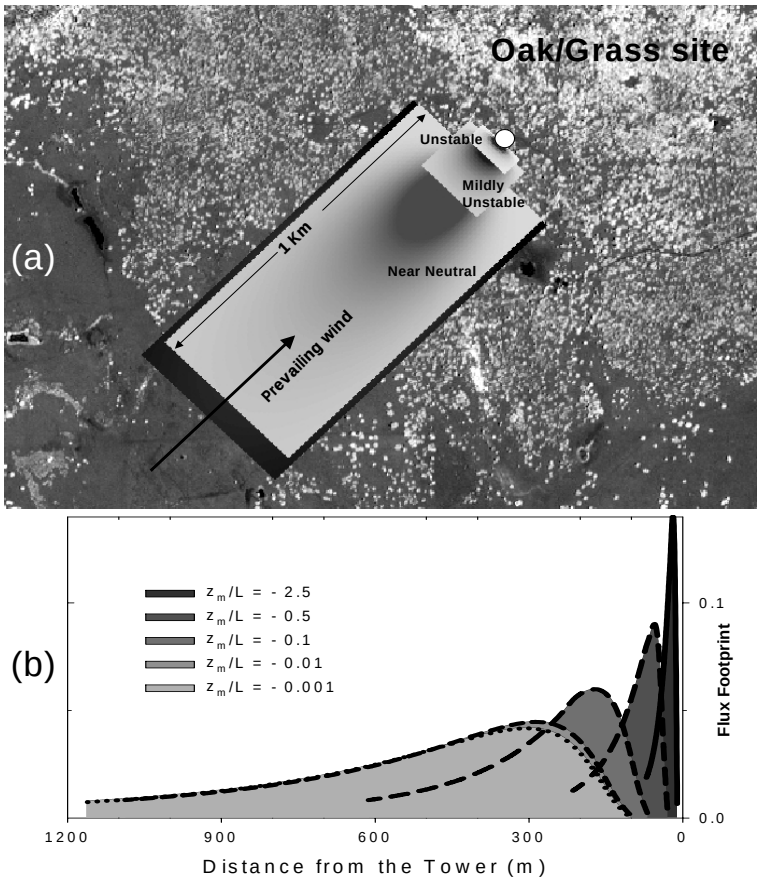

Figure 10 J. Kim and Q. Guo, analysts.

The combination of wind roses, remote sensing imagery and flux footprint computations enables us to compute the flux footprint for the site. Below is an intial computation performed by Peter Levy with several months of wind data.

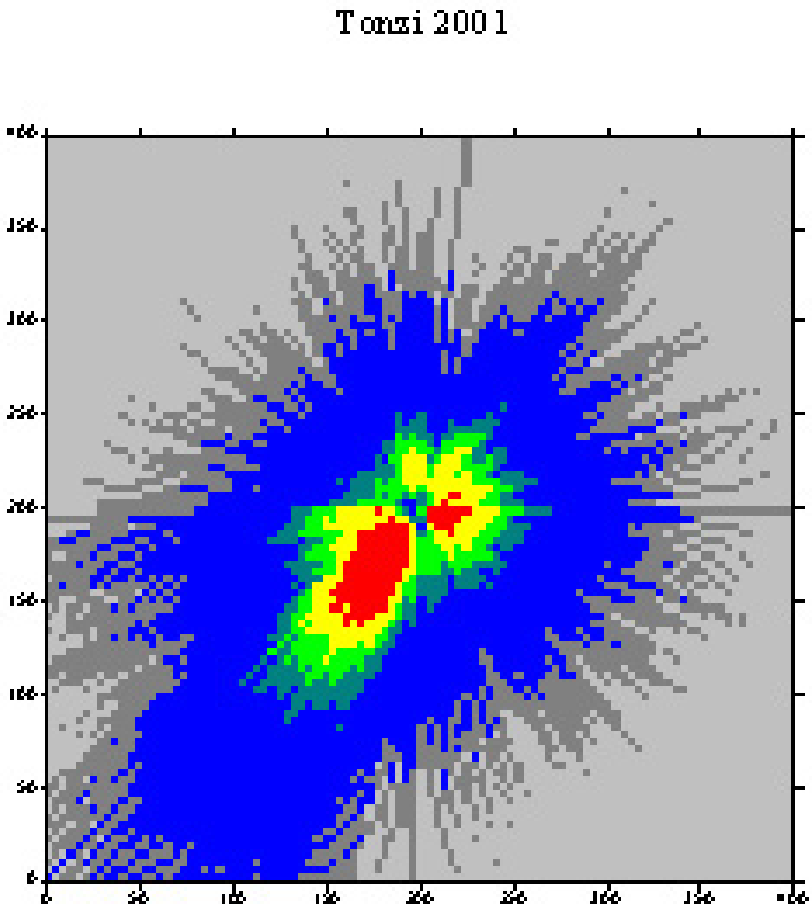

Figure 11 Flux footprint. Tonzi Ranch. Prepared by Peter Levy

6.2.2 Spatial Resolution.

NDVI at 4 m resolution was deduced from IKONOS images. The variance of the vegetation was assessed with different averaging windows, which follows a –0.4 power law.

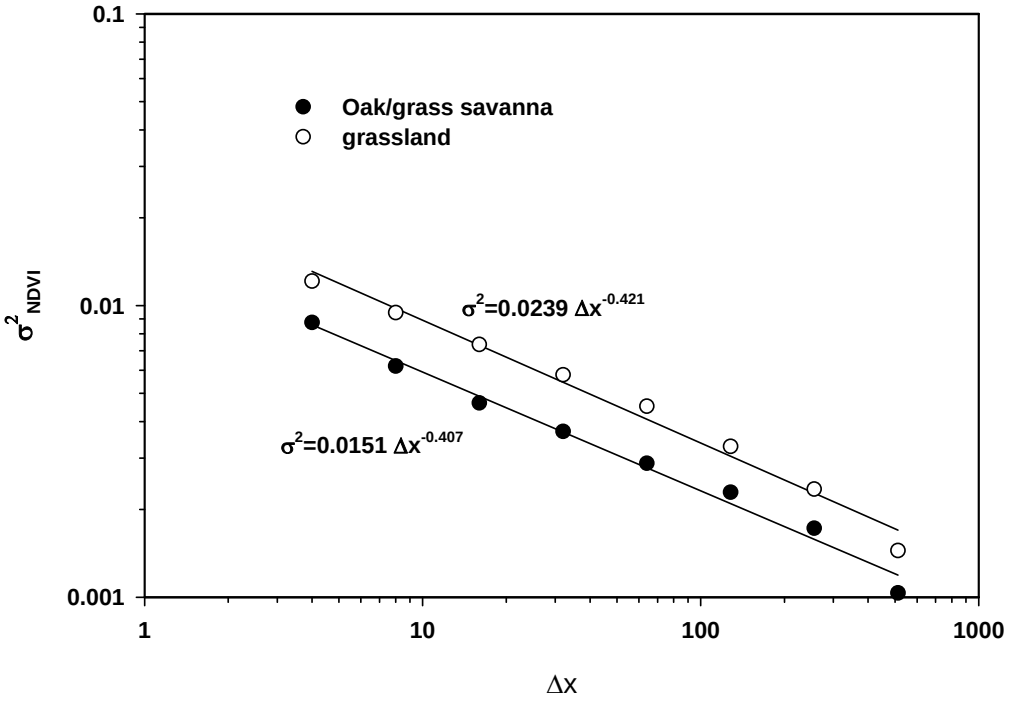

Figure 12 D. Baldocchi Analyst

Biogeography

The field site is located on the eastern side of the Sacramento Valley in the lower foothills of the Sierra Nevada mountains. This ecosystem is the oak savanna woodland (see Barbour and Minnich, California upland forests and woodlands, In: North American Terrestrial Vegetation, 2nd Editions, eds MG Barbour, WD Billings. 2000. Cambridge Univ Press. Pp 161-202.

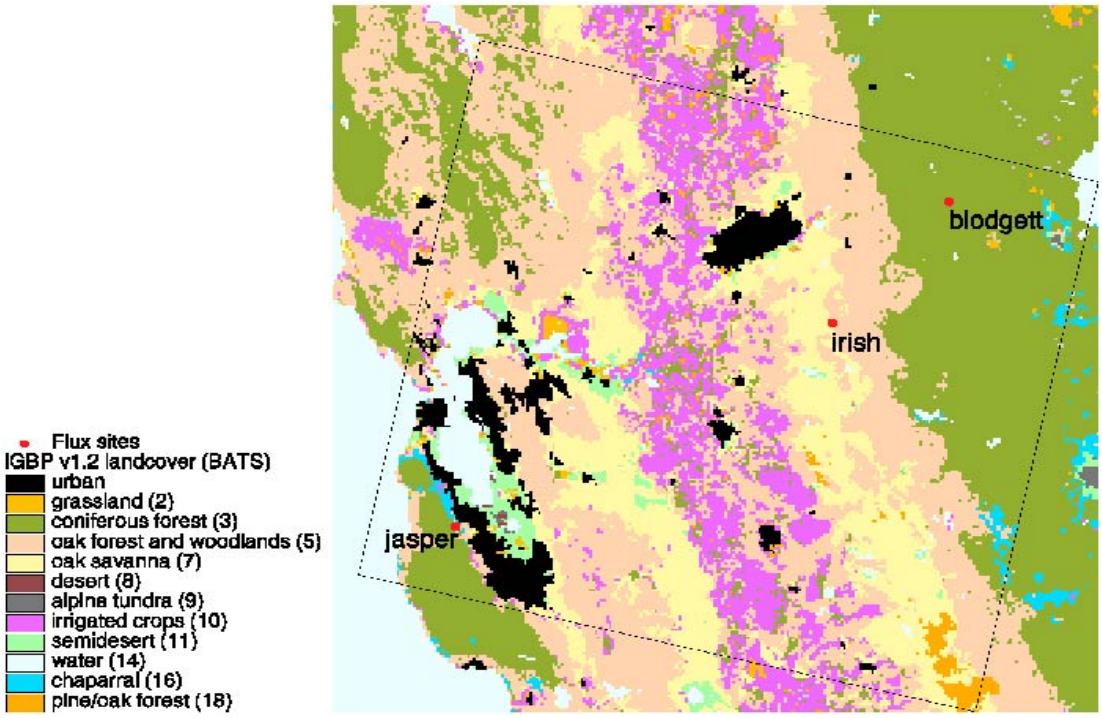

Figure 13 Regional distribution of ecosystems in Northern California, after Joe McFadden, Un Minn.

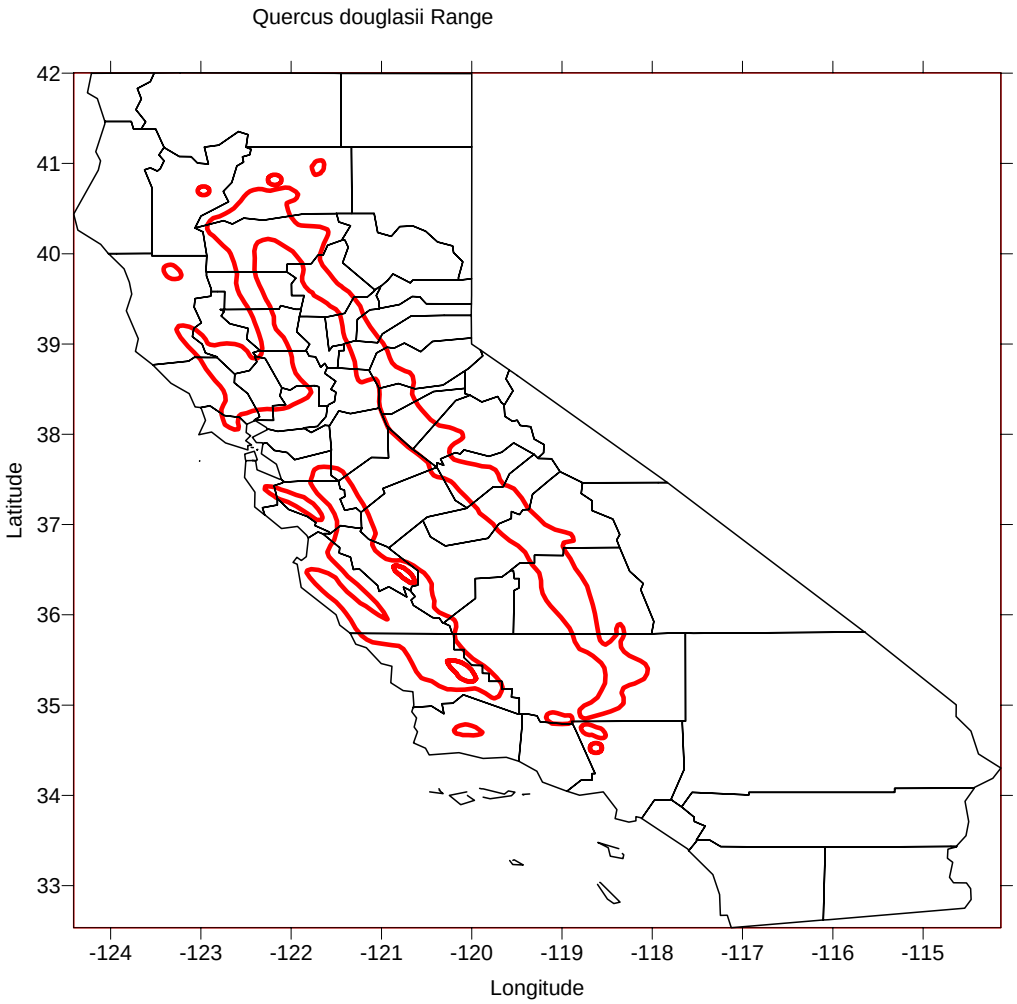

Figure 14 Blue Oak range in California

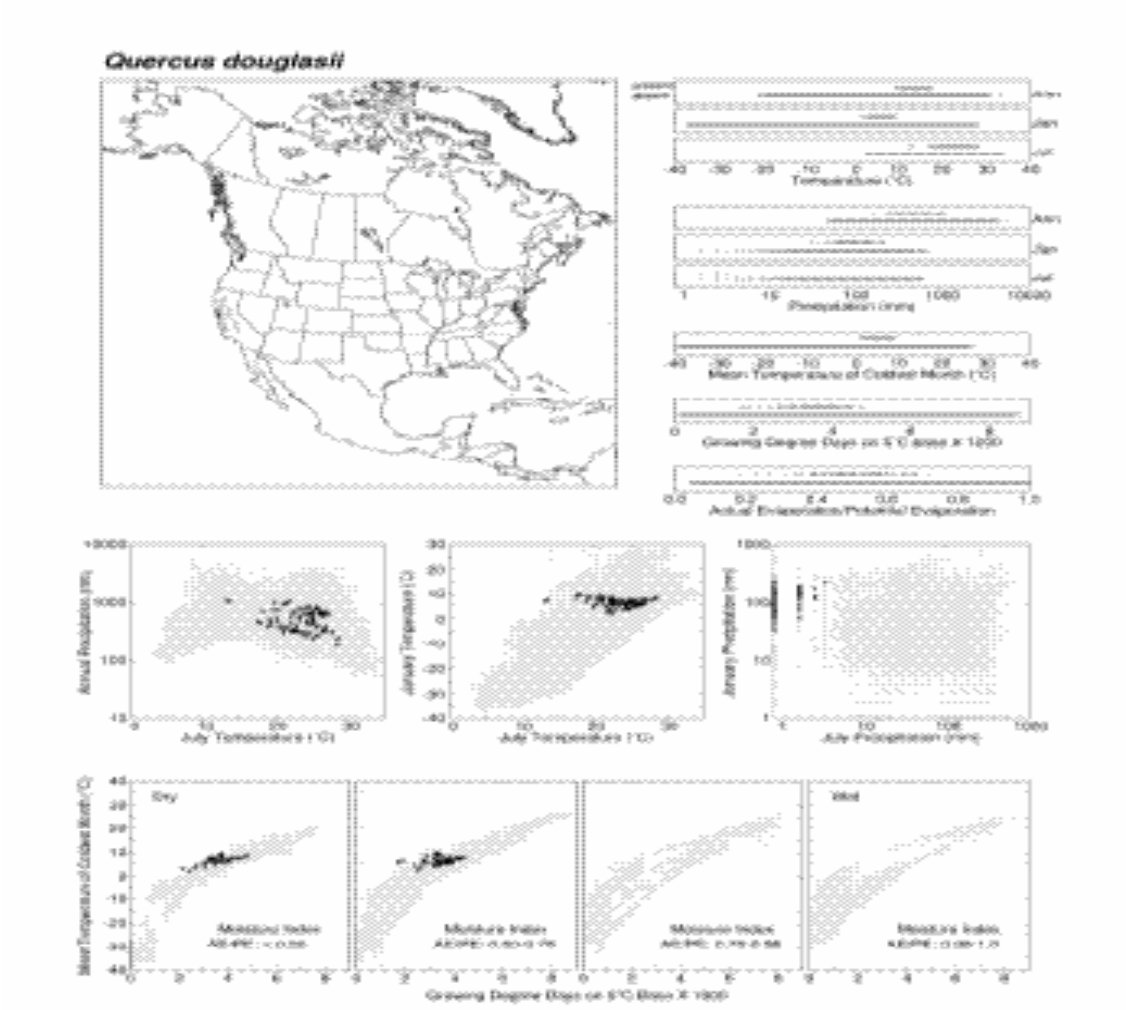

Figure 15 http://greenwood.cr.usgs.gov/pub/ppapers/p1650-a/pages/qudotrim.pdf

Topography

Topographical information are available from USGS, the DEM associated with the IKONOS image and from removing trees from the laser altimeter image (Chen et al.).

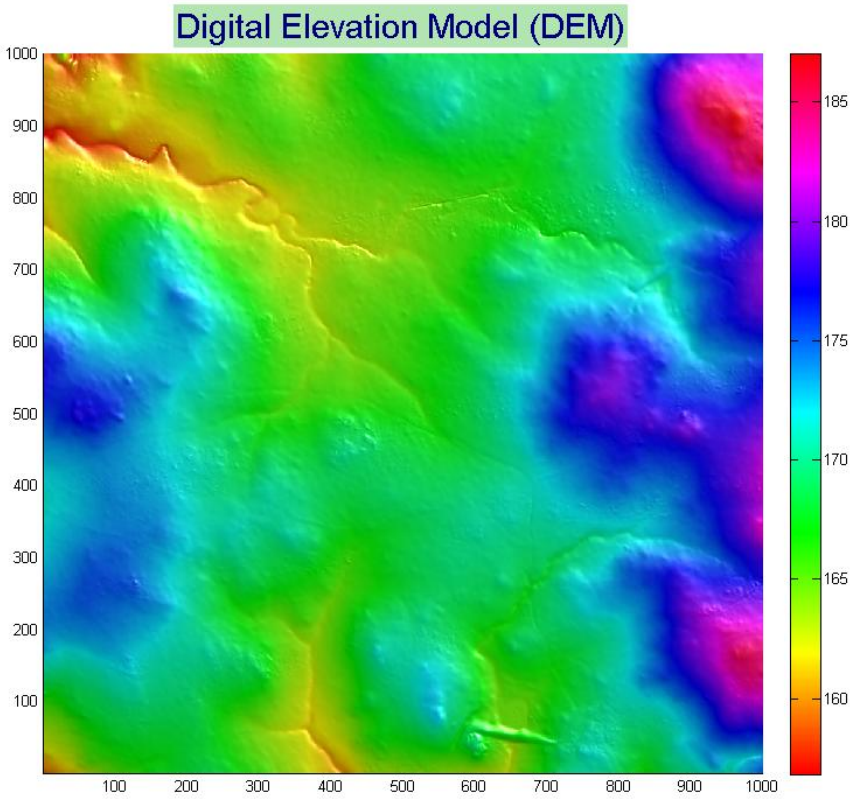

Figure 16 Digital elevation map of Tonzi ranch, derived from LIDAR data. Qi Chen, analyst.

Proposed Meteorological Tower Site, Tonzi Ranch, Ione, CA

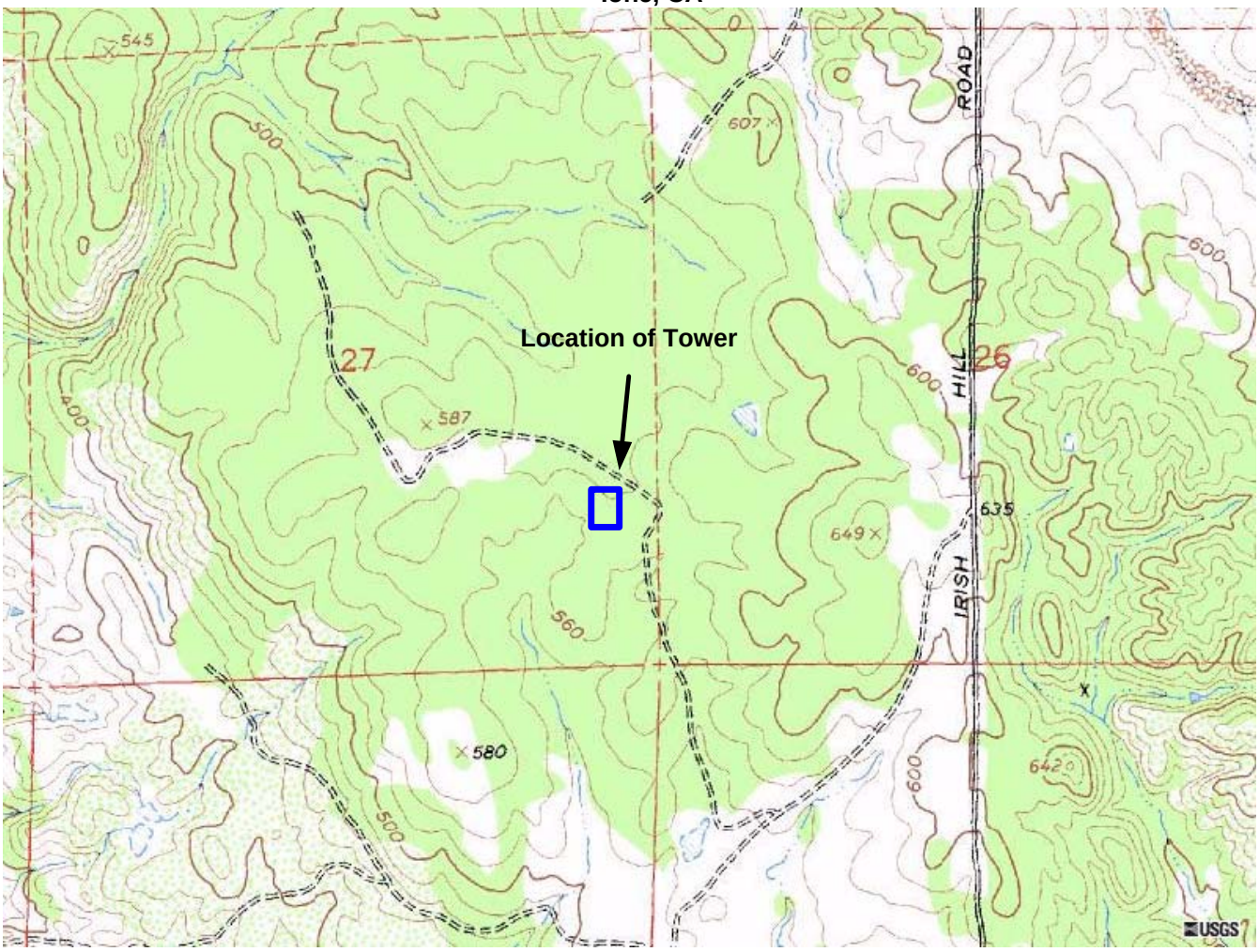

(see USGS 7.5' Quadrangle: Irish Hill, Calif.Sections 26, 27, 34, 35)

A. Site Characteristics

The site is a grazed oak/grass woodland. The landscape has been managed, as the local ranchers have removed brush and cattle graze the herbs. The main grass and herb species include bromus, frescue, oat, medusa head, rose clover. This an annual and seasonal grassland. The active growing season is between November and May.

Data from Lidar of savanna canopy

Individual Tree Metric	Mean	Std
Area(m2)	39.237	41.162
Radius(m)	3.1813	1.5392
Tree height(m)	9.4083	4.3348
Trunk height (m)	1.7504	1.3479
Crown height (m)	7.6579	4.5646
Basal area (m2)	0.07435 2	0.08394 2
Stem volume (m3)	0.73436	1.2331
Stem biomass (kg)	440.43	739.56
Leaf area (m2)	38.326	64.357
LAI	0.70599	0.40827

LAI data of the overstory was collected by Nancy Kiang, using the LI-2000 and by litterbags collected by John Battles group. The LAI of the understory was sampled periodically by Xu and Baldocchi.

Date	Jday	LAI_Overstory	Date	DOY	LAI_Understory
15-Mar	74	0	6-Jan	6	0.49
23-Mar	82	0.45	23-Feb	54	0.45
10-May	130	0.66	8-Mar	67	0.46
23-May	143	0.65	22-Mar	81	0.5
6-Jun	157	0.66	8-Apr	98	0.84
5-Jul	186	0.63	18-Apr	108	0.93
20-Jul	201	0.65	3-May	123	0.86
1-Aug	213	0.65	17-May	137	0
11-Sep	254	0.61			

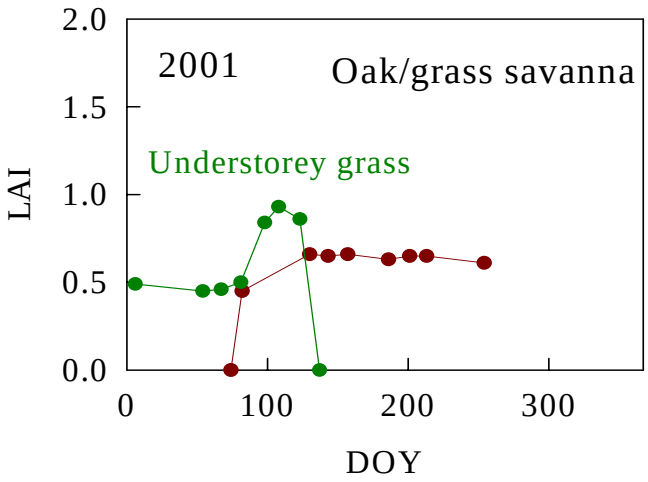

Figure 17 Lai seasonal trend for over and understorey

More recently, we have been assessing tree coverage with remote sensing acquisitions (IKONOS, Lidar Altimeter).

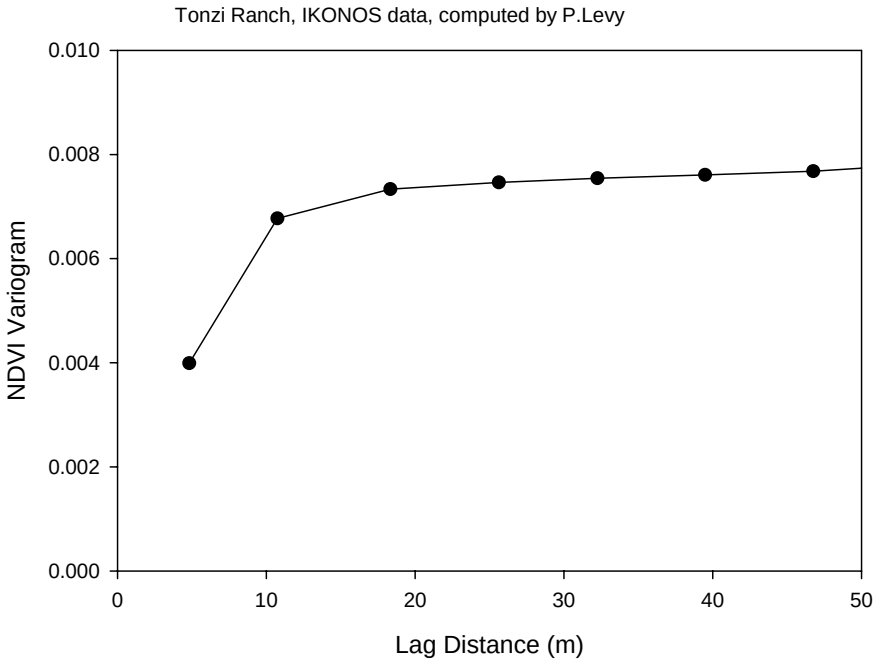

Figure 18 Lag Correlation of NDVI from IKONOS Image. Produces information on the scale of gaps in the canopy. They tend to be less than 10 m.

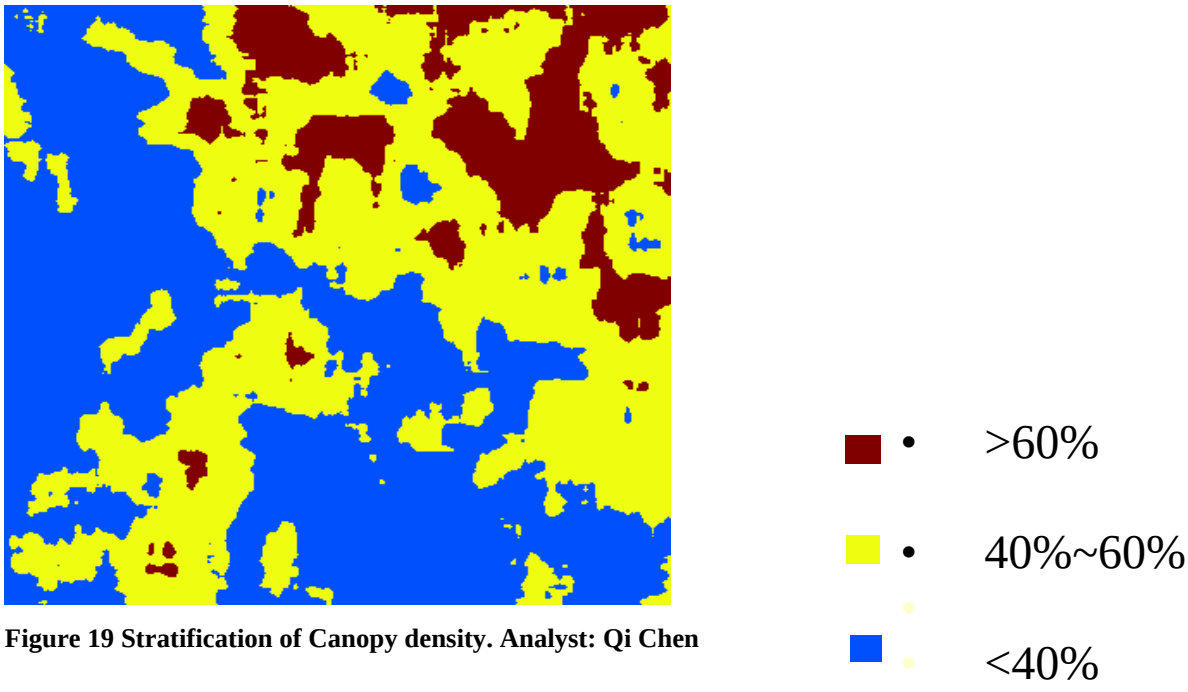

Figure 19 Stratification of Canopy density. Analyst: Qi Chen

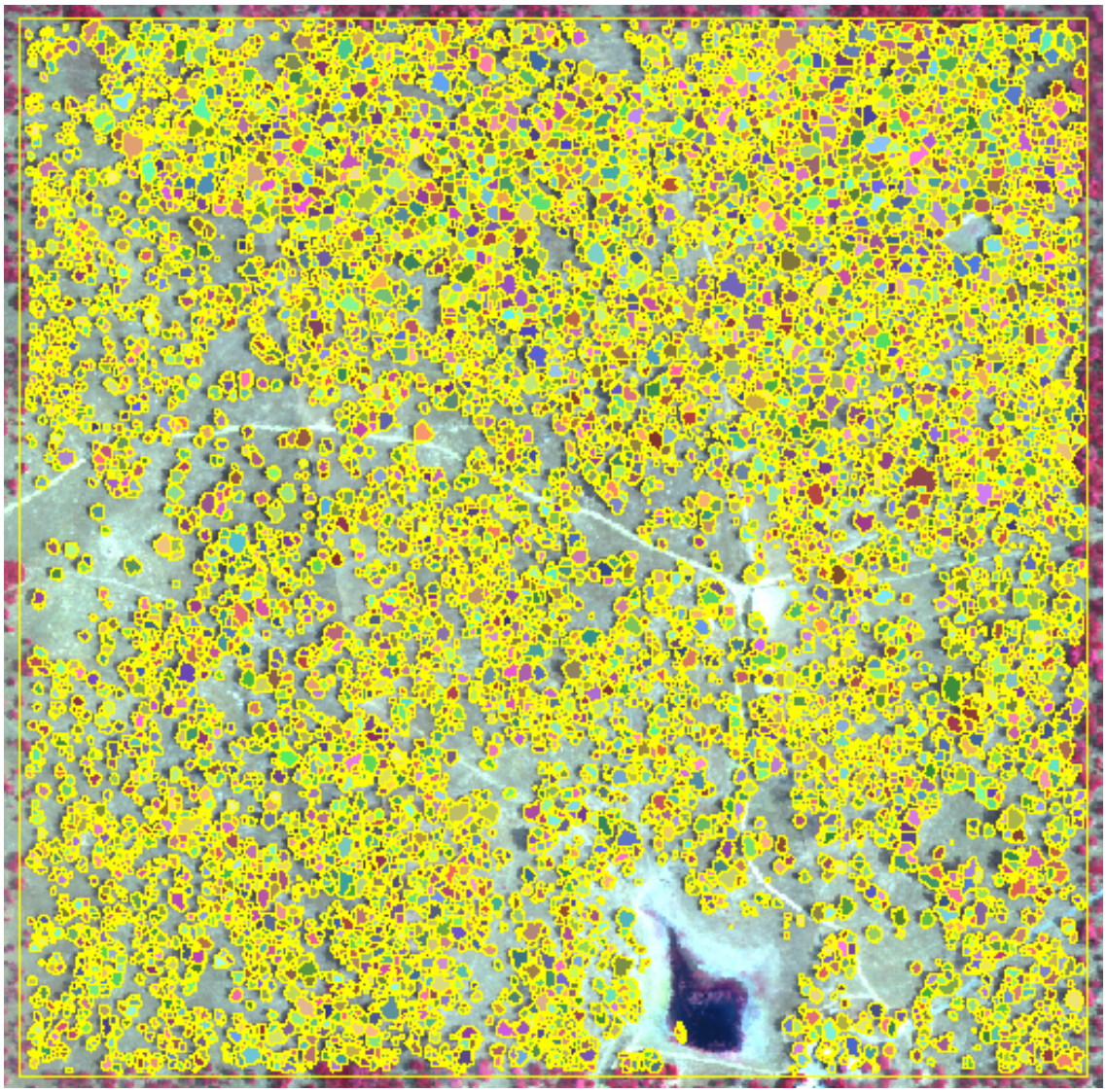

Figure 20 Mapping of trees around tower site. Qi Chen analyst. LIDAR data

Working with the MODIS project, colleagues have assessed the representativeness of our site with respect to the larger region, 7 by 7 km.

9	9	8	8	8	9	9
8	9	8	8	8	9	9
9	8	9	8	8	9	8
9	9	9	8	8	8	9
9	10	9	9	9	9	2
8	8	9	9	9	9	9
8	7	8	9	9	6	8

Figure 21 7 by 7 km Modis cutout around the Tonzi Tower. Faith Anne Heinsch, U Mt, analyst

Code
2: evergreen broadleaved forest
6: closed shrubland
7: open shrubland
8: woody savanna
9: savanna
10: grassland

SOILS

Information on soils come from the Soil Survey of Amador Area, California, 1965, USDA. The soil is of the Auburn-Exchequer association. It is a very shallow to moderately deep rocky or gravely soil in material from metabasic rocks and metasedimentary slate and schist (Soil Survey of Amador Area, California, 1965, USDA, Soil Conservation Service)

Classified as AsD, Auburn extremely rocky silt loam, 3 to 31 percent slopes. The profile is:
*0-9 inches, strong brown silt loam, Massive. Hard when dry, friable when wet slightly acid
*9-14 inches yellowish red silt loam. Massive. Hard when dry, friable when wet, slightly acid.
*14 inches plus, weathered, very pale brown

AUBURN SERIES

The Auburn series consists of shallow to moderately deep, well drained soils formed in material weathered from amphibolite schist. Auburn soils are on foothills and have slopes of 2 to 75 percent. The mean annual precipitation is about 24 inches and the mean annual temperature is about 60 degrees F.

TAXONOMIC CLASS: Loamy, mixed, superactive, thermic Lithic Haploxerepts

AUBURN

Date SC Updated: 08-MAR-01

MO Responsible: 2 (DAVIS, CALIFORNIA)

State Type Location: CA

Series Status: E

Classification

Subgroup

Soil Order: INCEPTISOLS

Suborder: XEREPTS

Great Group: HAPLOXEREPTS

Subgroup Modifier: LITHIC

Family

Particle Size: LOAMY

Particle Size Modifier:

Mineralogy: MIXED

CEC Activity: SUPERACTIVE

Reaction:

Soil Temperature: THERMIC

Other:

TYPICAL PEDON: Auburn silt loam - on an east facing slope of 10 percent under annual grass, oak and digger pine at 620 feet elevation. (Colors are for dry soil unless otherwise stated. When described on March 27, 1959, the soil was dry throughout.)

A1--0 to 1.5 inches; strong brown (7.5YR 5/6) silt loam, reddish brown (5YR 4/4) moist; massive; slightly hard, friable, slightly sticky and nonplastic; many very fine roots; many very fine and fine tubular pores; slightly acid (pH 6.4); clear smooth boundary. (1 to 8 inches thick)
A2--1.5 to 9 inches; yellowish red (5YR 5/6) silt loam, reddish brown (5YR 4/4) moist; massive; slightly hard, friable, slightly sticky and slightly plastic; many very fine and medium roots; many very fine and medium tubular pores; slightly acid (pH 6.4); gradual smooth boundary. (1 to 8 inches thick)
Bw--9 to 14 inches; yellowish red (5YR 5/8) silt loam, yellowish red (5YR 4/6) moist; massive; slightly hard, friable, slightly sticky and slightly plastic; many very fine roots; many very fine tubular pores; few thin clay films line pores; slightly acid (pH 6.5); abrupt wavy boundary. (5 to 12 inches thick)
R--14 to 24 inches; very pale brown (10YR 7/4) partly weathered amphibolite schist with reddish brown (2.5YR 4/4) colloidal stains in fracture planes; few roots in cracks; slightly acid (pH 6.5).
TYPE LOCATION: Amador County, California. About 3.5 miles northeast of Ione, 0.25 miles east and 100 feet north of the southeast corner of sec. 6 T. 6 N, R. 10 E. Irish Hill Quadrangle.

http://www.statlab.iastate.edu/soils/osd/dat/A/AUBURN.html

capability units Vis-4 (18) range site 2.

The soil bulk density in the open was assessed from a random field sampling design.

1.64 +/- 0.107 g cm^{-3}, based on 27 samples from 5 to 30 cm

Under the trees

1.58 +/- 0.136 g cm-3

Soil Water Retention Curve

Soil pressure (atmospheres)	open	Under canopy
.3	17.8	19.4
1	14.7	15.1
5	13.4	13.4
10	8.5	8.55
15	8.2	7.95

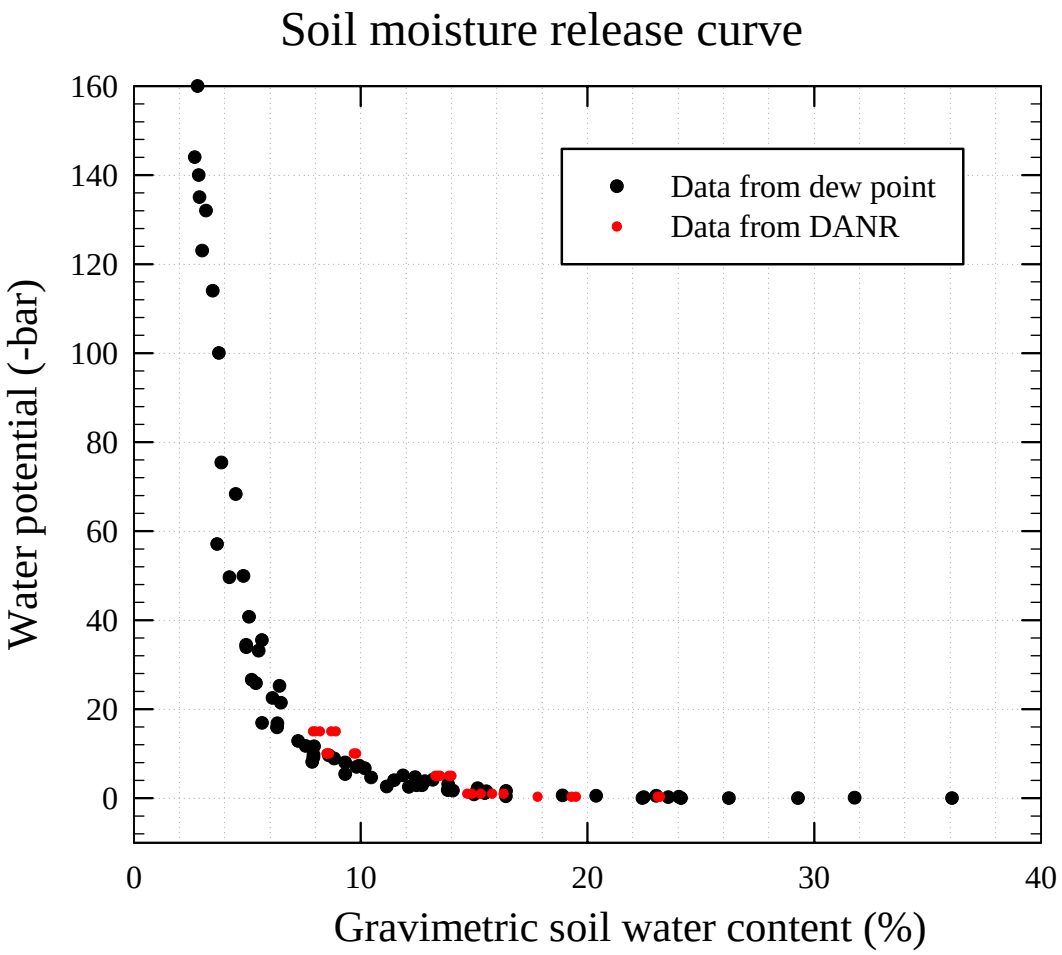

Figure 22 soil Moisture Retention curve with Decagon Dewpoint hygrometer, Xu et al. Also plotted on the curve are the data from DANR

Soil Texture

	Sand	Silt	Clay
DESC	%	%	%
Under Canopy	38	45	17
Under Canopy	37	45	18
Open Space	48	42	10

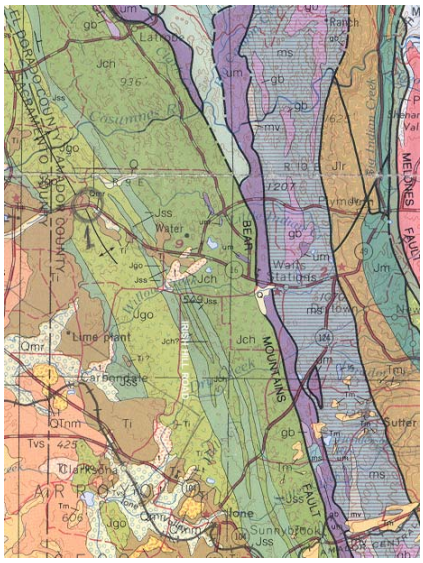

Figure 23 Geological soils map for the Ione, CA area near the Tonzi and Vaira ranches

Soil thermal conductivity was determined with the amplitude method documented in Verhoef et al. AT this site it varies with time and soil moisture

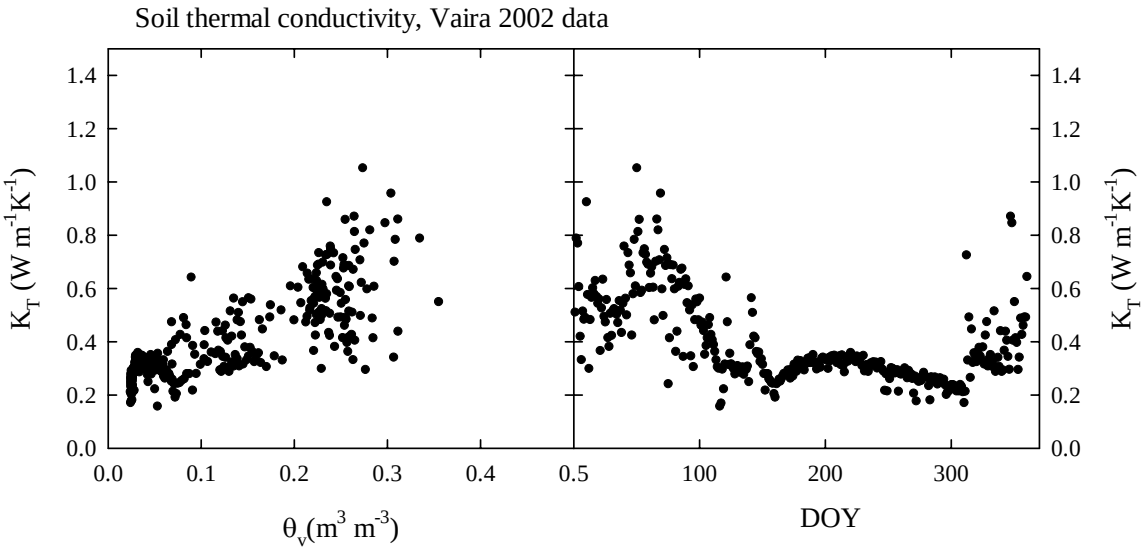

Soil thermal conductivity (K_T) as a function of volumetric soil water content (θ_v), and its seasonal variations in 2002 at Vaira grassland. K_T was calculated as the products of heat capacity (C_p) and thermal diffusivity (λ). λ was obtained based on the amplitudes of soil temperature at depths of 2 and 4 cm.

Soil Chemistry

Soil chemistry was determined on samples processed at UC Davis DANR soil Lab

	N-TOT	C-Tot	C-N
DESC	%	%	
Underc			10.3
canopy	0.11	1.13	
Underc			9.6
canopy	0.11	1.06	
Open Space	0.10	0.92	9.2

In 2006, extensive soil surveys were conducted by Gretchen Miller and Xingyuan Chen

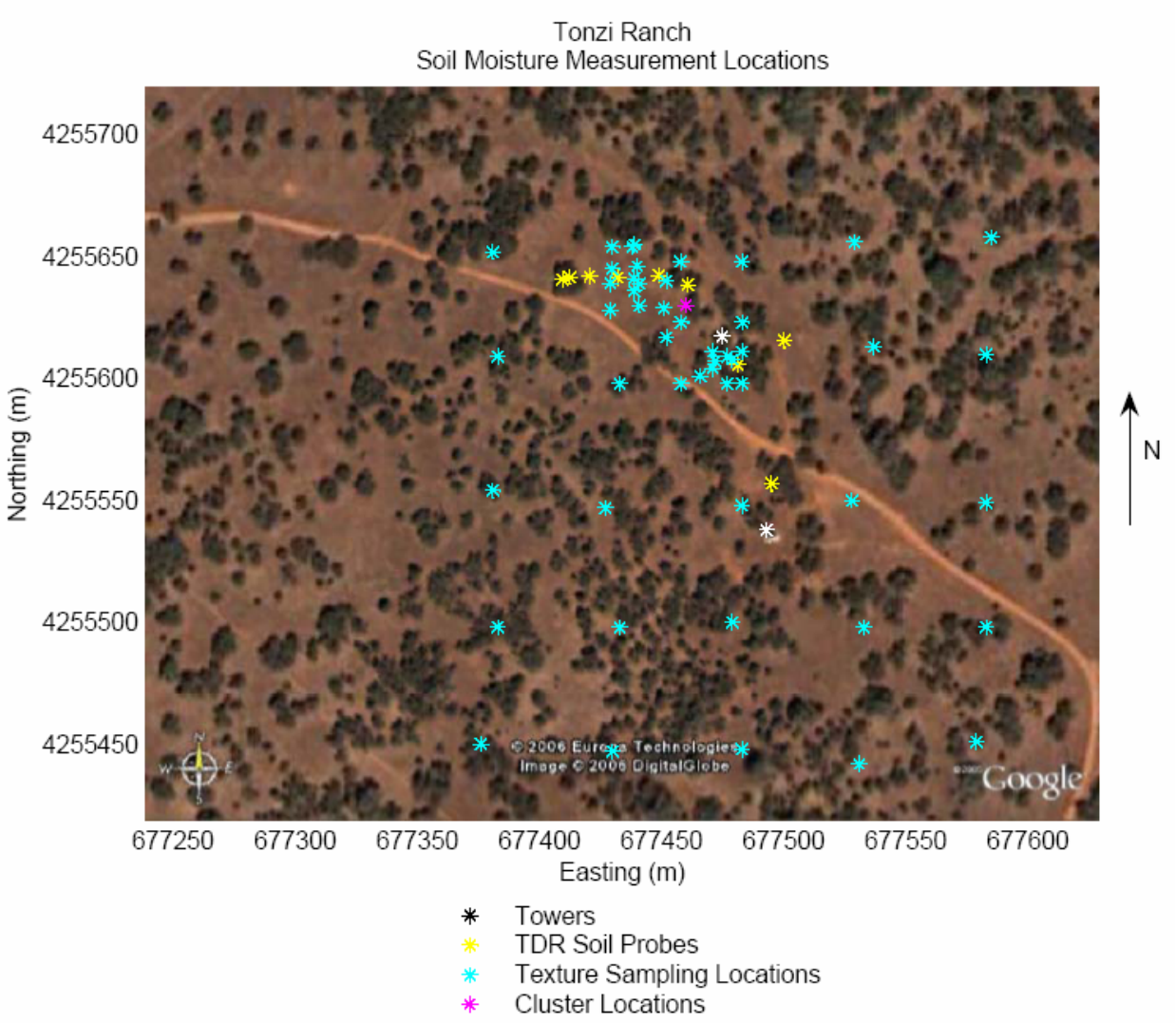
Tonzi Ranch
Soil Moisture Measurement Locations
Northing (m)
4255700
4255650
4255600
4255550
4255500
4255450
677250
677300
677350
677400
677450
677500
677550
677600
Easting (m)
N
© 2006 Eurosa Technologies
Image © 2006 DigitalGlobe
Google
Towers
TDR Soil Probes
Texture Sampling Locations
Cluster Locations

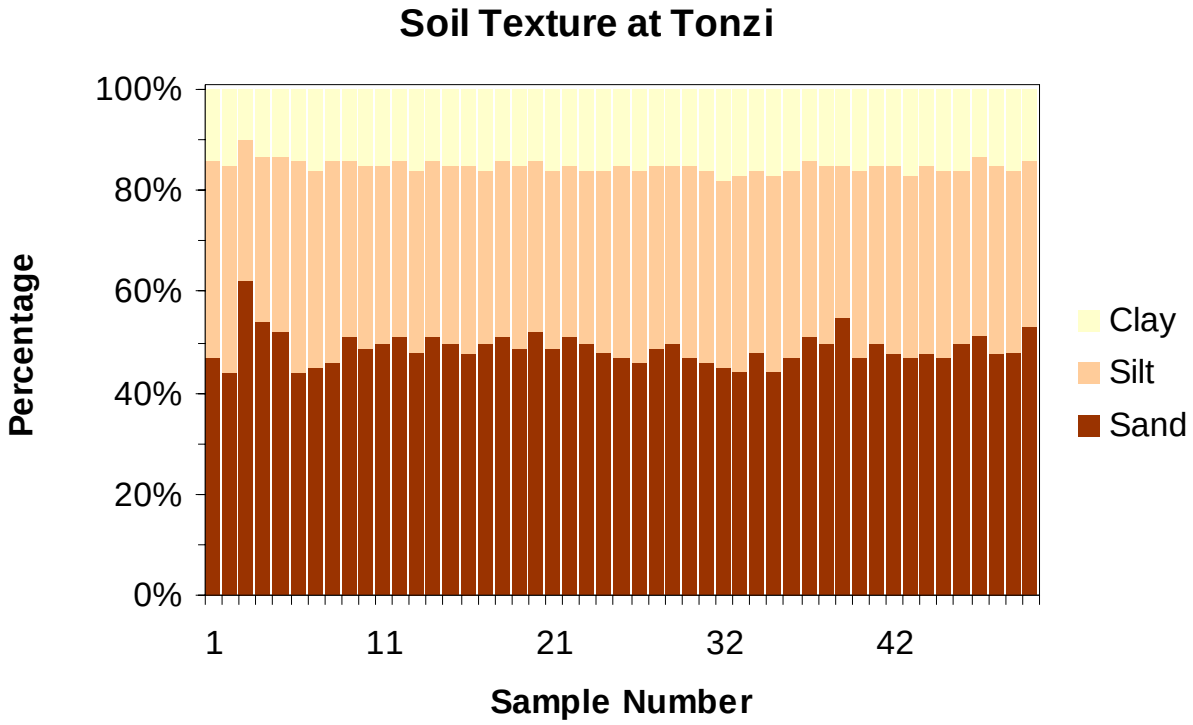
Soil Texture at Tonzi
100%
80%
60%
40%
20%
0%
Percentage
1
11
21
32
42
Sample Number
Clay
Silt
Sand

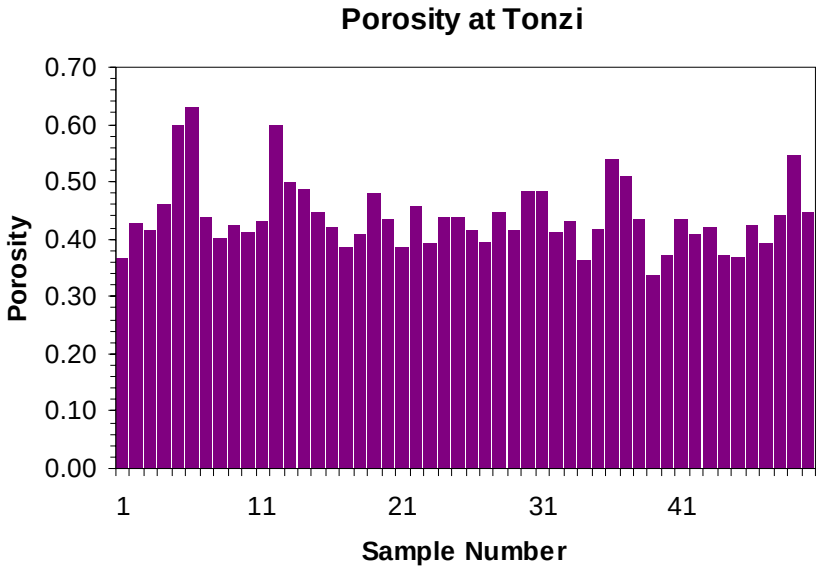
Porosity at Tonzi
0.70
0.60
0.50
0.40
0.30
0.20
0.10
0.00
Porosity
1
11
21
31
41
Sample Number

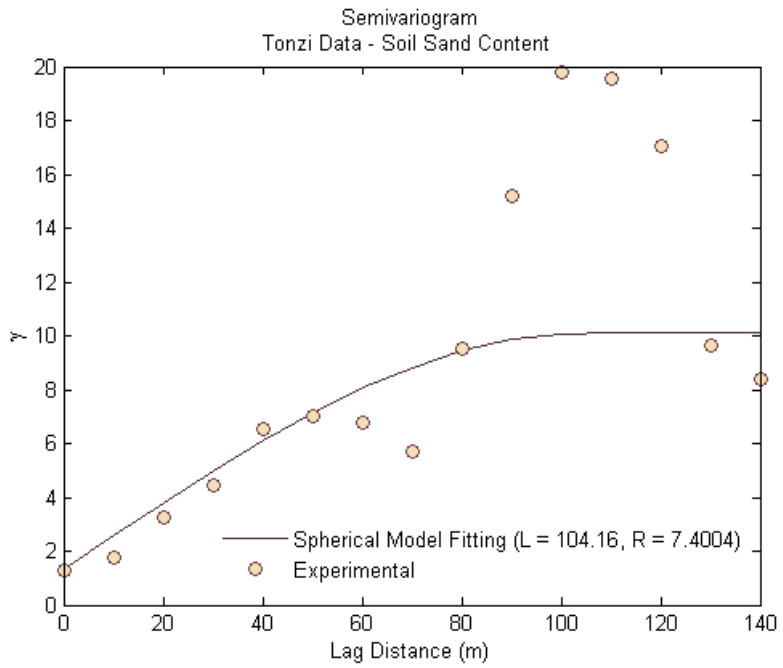
Semivariogram
Tonzi Data - Soil Sand Content
γ
Lag Distance (m)
Spherical Model Fitting (L = 104.16, R = 7.4004)
Experimental
0
2
4
6
8
10
12
14
16
18
20
0
20
40
60
80
100
120
140

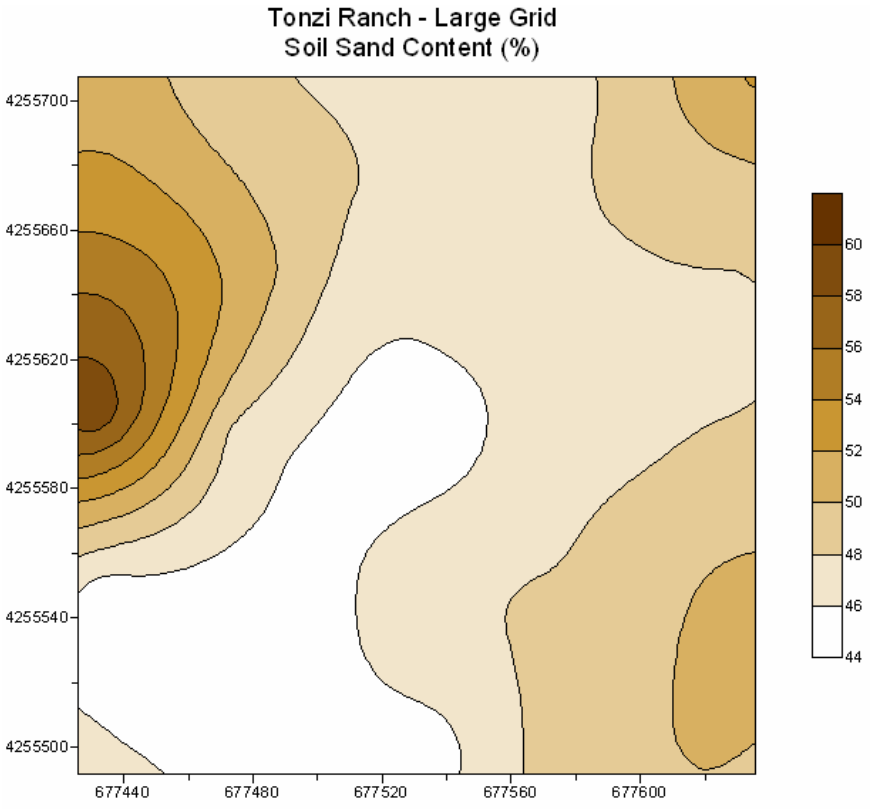
Tonzi Ranch - Large Grid
Soil Sand Content (%)
4255700
4255660
4255620
4255580
4255540
4255500
677440
677480
677520
677560
677600
60
58
56
54
52
50
48
46
44

Climate

There is no direct climate data from the ranches under investigation, but there is climate information in the region. There is a discontinued cooperative weather station in Ione, that gives us rain data between 1959 and 1977.

There is no long term weather records at the site, but weather records from are available from the NCDC cooperative network for Ione, from 1959-1977 (t *about* 38.35°N 120.93°W. Height *about* 85m / 278 feet above sea level)

Ione

Average Rainfall

	Jan	Feb	Mar	Apr	May	Jun	Jul	Aug	Sep	Oct	Nov	Dec	Year
mm	99.6	83.9	76.8	51.9	10.7	3.1	0.3	5.2	5.5	31.6	94.5	94.6	558.7
inches	3.9	3.3	3.0	2.0	0.4	0.1	0.0	0.2	0.2	1.2	3.7	3.7	22.0

Source: derived from NCDC Cooperative Stations. 16 complete years between 1959 and 1977 a near by station, Ben Bolt, recorded

There is a weather station at Pardee dam, which is south of the site, but on a similar altitudinal gradient, so the annual temperatures and rainfall sums are close.

CAMP PARDEE, CALAVERAS COUNTY, CALIFORNIA USA

Located at *about* 38.25°N 120.86°W. Height *about* 200m / 656 feet above sea level.

Average Temperature

	Jan	Feb	Mar	Apr	May	Jun	Jul	Aug	Sep	Oct	Nov	Dec	Year
°C	7.3	10.0	11.6	14.5	18.5	22.6	25.8	25.1	22.6	18.3	12.1	7.8	16.3
°F	45.1	50.0	52.9	58.1	65.3	72.7	78.4	77.2	72.7	64.9	53.8	46.0	61.3

Source: derived from NCDC TD 9641 Clim 81 1961-1990 Normals. 30 years between 1961 and 1990

CAMP PARDEE, CALAVERAS COUNTY, CALIFORNIA USA

Located at *about* 38.25°N 120.86°W. Height *about* 200m / 656 feet above sea level.

Average Rainfall

	Jan	Feb	Mar	Apr	May	Jun	Jul	Aug	Sep	Oct	Nov	Dec	Year
mm	97.8	88.2	91.6	49.0	18.5	5.9	1.2	1.6	8.5	29.5	65.5	85.4	543.7
inches	3.9	3.5	3.6	1.9	0.7	0.2	0.0	0.1	0.3	1.2	2.6	3.4	21.4

Source8.0) DATA DESCRIPTION

Note the Pardee rainfall is 543 mm while the discontinued Ione site produced a mean of 558 mm per year. Hence we feel that the Pardee climate is representative of this site.

In order to relate our data with other sites we include figures of Northern California rainfall.

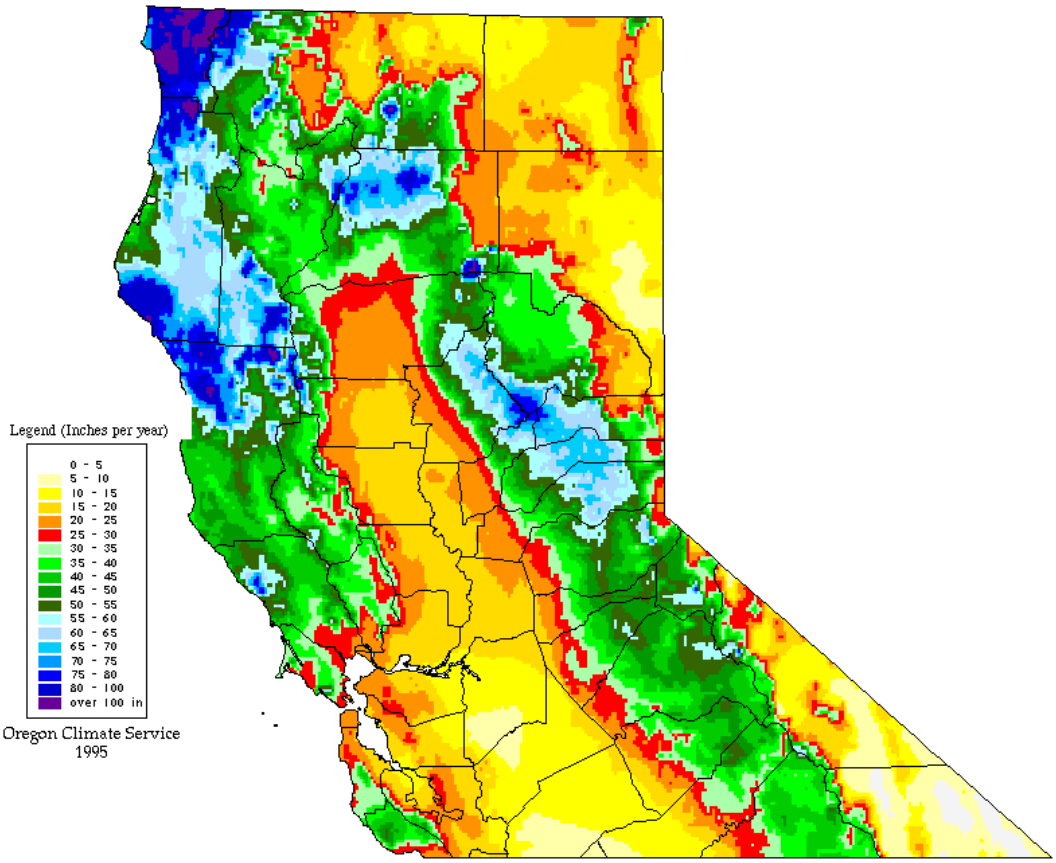

Figure 24 source http://www.wrh.noaa.gov/Monterey/CA_NORTH.GIF

Using interpolation calculations of regional climate data using MtCLIME (Peter Thorton, NCAR; http://www.daymet.org/) we estimate that a 30 year mean of precipitation is about 611 mm. The mean maximum temperature is 22.2663, the mean minimum temperature is 8.0207 and the mean annual temperature is 18.3492

Climate Reconstructions, courtesy of David Price

ANUSPLIN is a well-established and widely used statistical climate interpolator developed by Mike Hutchinson and colleagues at ANU in Canberra. see: http://cres.anu.edu.au/outputs/anusplin.php

My colleague Dan McKenney has worked with Mike closely for several years and is our (Canadian Forest Service) guru on climate data interpolation.

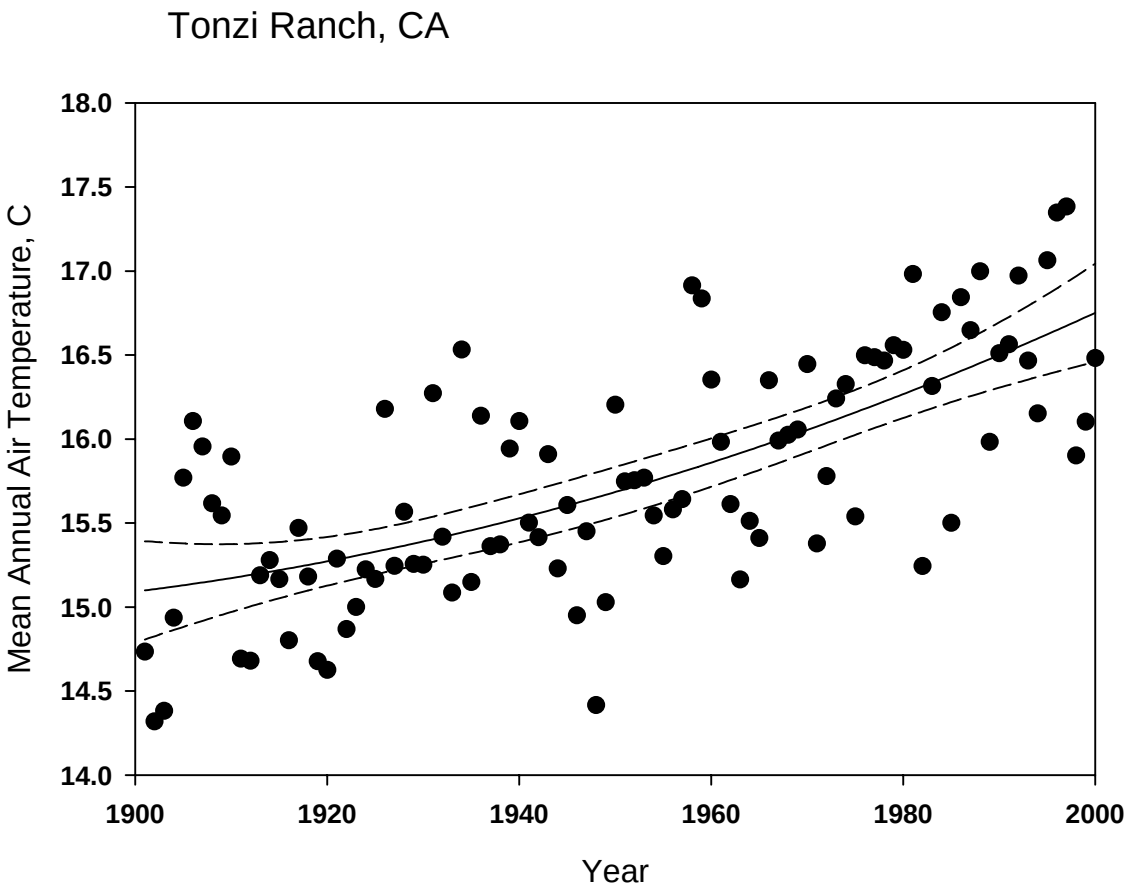

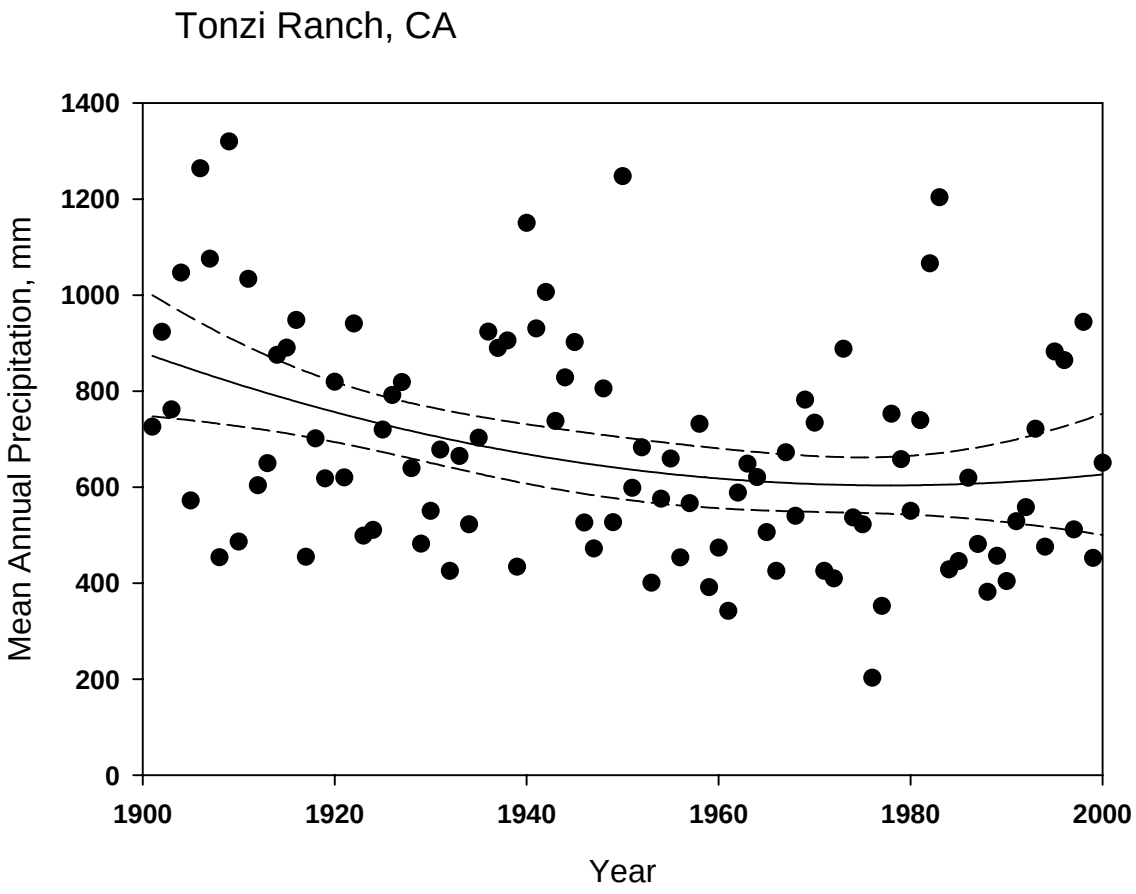

We have now collected several years of radiation measurements and can produce summaries of solar radiation at the site

Table 2 Energy Climatology at the Grass and Savanna sites

	Grassland 2001	**Grassland 2002**	**Oak Woodland 2002**
E (mm yr^{-1})	299	290	381
E_{eq} (mm yr^{-1})	568	601	864
ppt (mm)	556	494	494
R_n (GJ m^{-2} $yr^{-1)}$	2.11	2.29	3.25
ppt/E	1.85	1.70	1.29

Ppt/E_{eq}	0.98	0.82	0.57

Wind roses have been computed too. They reflect drainage winds at night from the Sierra Nevada mountains to the east. During the day winds tend to come from the south west reflecting flow in from the Delta, or from the North west, as fronts pass or High pressure ridges set up.

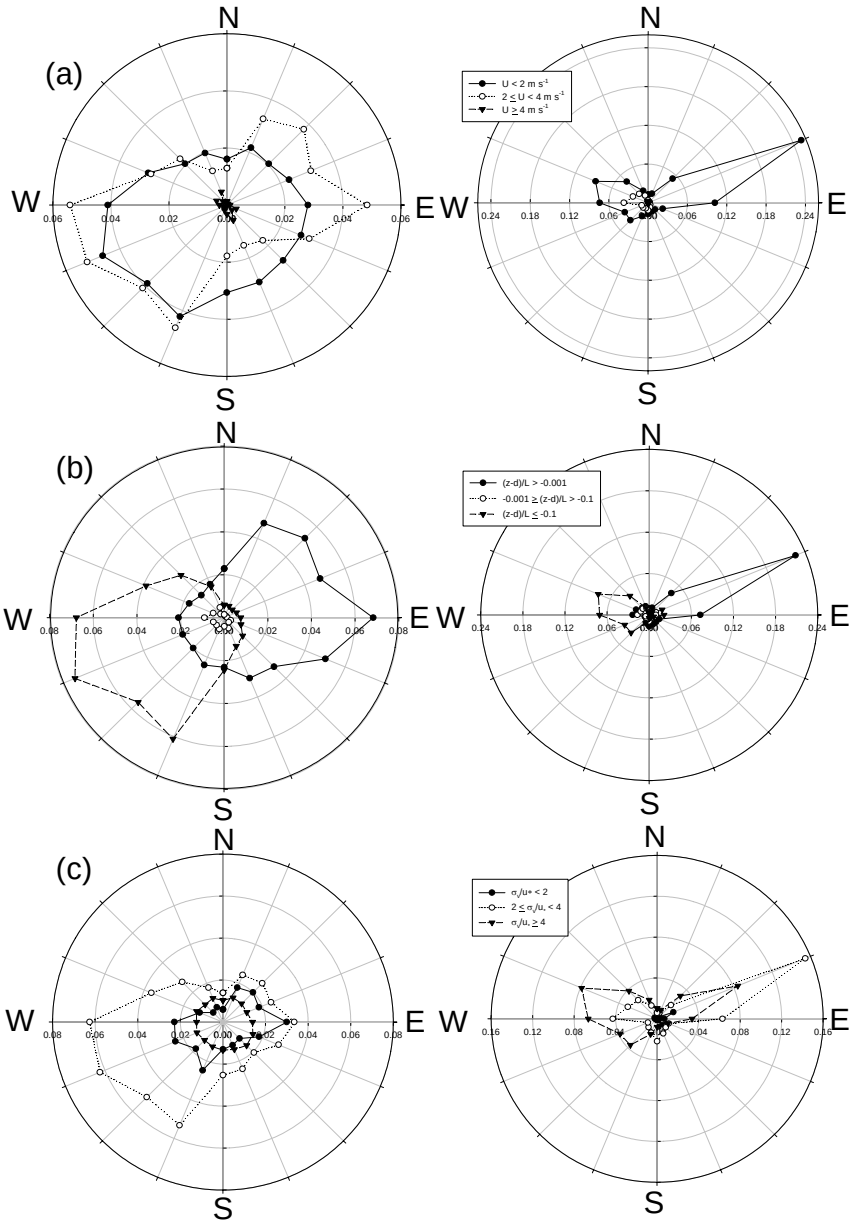

Figure 25 Wind rose climatology. J. Kim, analyst

Plant Structure and Function

The Tonzi ranch consists of scattered blue oak trees (Quercus douglasii) and grey pine. Figure 26 is a close up picture of a blue oak leaf. Typical leaf size is XXX mm.

Figure 26 Upclose picture of blue oak leaf

During the spring of 2001, the Ecology group of Dr. John Battles assessed the species composition of the underlying grass.

Species abundance of the understory
Data of John Battles, Randy Jackson and students

GENUS	SPECIES	FAMILY	CODE	Frequency	% total
Brachypodium	distachyon	Poaceae	BRDI2	225	34.09%
OAK LITTER			OL	75	11.36%
Hypochaeris	glabra	Asteraceae	HYGL	68	10.30%
Bromus	madritensis	Poaceae	BRHO	63	9.55%
LITTER			L	55	8.33%
Cynosurus	echinatus	Poaceae	CYEC	33	5.00%
Aira	caryophyllea	Poaceae	AICA	31	4.70%
Vulpia	myuros	Poaceae	VUMY	22	3.33%
BARE			B	12	1.82%
Trifolium	dubium	Fabaceae	TRDU	12	1.82%
Briza	minor	Poaceae	BRMI	10	1.52%
Bromus	diandrus	Poaceae	BRDI	7	1.06%
Bromus	hordeaceus	Poaceae	BREL	7	1.06%
Trifolium	hirtum	Fabaceae	TRHI	5	0.76%
Briza	maxima	Poaceae	BRMA	4	0.61%
Calochortus	species	Liliaceae	CALOCHOR	3	0.45%

Unknown	forb 1		UKF1	3	0.45%
Aegilops	triuncialis	Poaceae	AETR	2	0.30%
Centaurea	melitensis	Asteraceae	CEME	2	0.30%
Dichelostemma	volubile	Liliaceae	DIVO	2	0.30%
Gastridium	ventricosum	Poaceae	GAVE	2	0.30%
Juncus	bufonius	Juncaceae	JUBU	2	0.30%
Nassella	pulchra	Poaceae	NAPU2	2	0.30%
Quercus	douglasii	Fagaceae	QUDO	2	0.30%
Sanicula	bipinnatifida	Apiaceae	SABI	2	0.30%
Sherardia	arvensis	Rubiaceae	SHAR	2	0.30%
Avena	barbata	Poaceae	AVBA	1	0.15%
Chlorogalum	pomeridianum	Liliaceae	CHPO	1	0.15%
Erodium	botrys	Geraniaceae	ERBO	1	0.15%
Linanthus	ciliatus	Polemoniaceae	LICI	1	0.15%
Madia	subspicata	Asteraceae	MASU	1	0.15%
Micropus	californicus	Asteraceae	MICA	1	0.15%
Plantago	erecta	Plantaginaceae	PLER	1	0.15%

Numerous studies are underway at the site to characterize tree height, distribution and functioning. The average from Nancy Kiang's transect studies show that the mean tree height is:

Mode: 8.6 m
Mean: 7.1
Max: 13.0 m

Using LIDAR data for a 1 km by 1 km scene, the mean values for tree height, trunk height, and crown radii are 10.1m, 1.5m, and 2.8m, respectively, and their standard deviations are 4.7m, 1.6m, and 1.6m, respectively. The validation for these parameters is still ongoing.

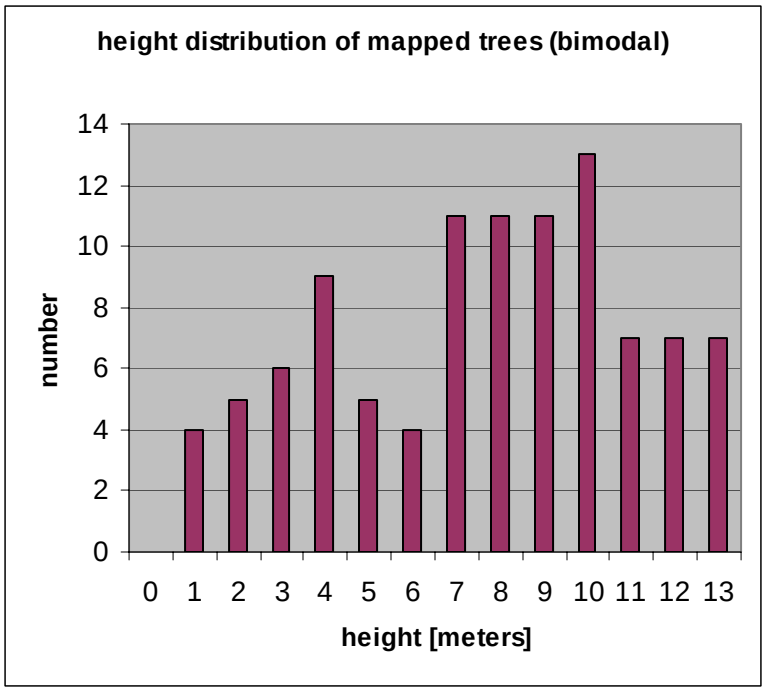

Figure 27 Data of Nancy Kiang

The diameter at Breast height is:

Mean 22.1 cm
Mode: 19.9 cm

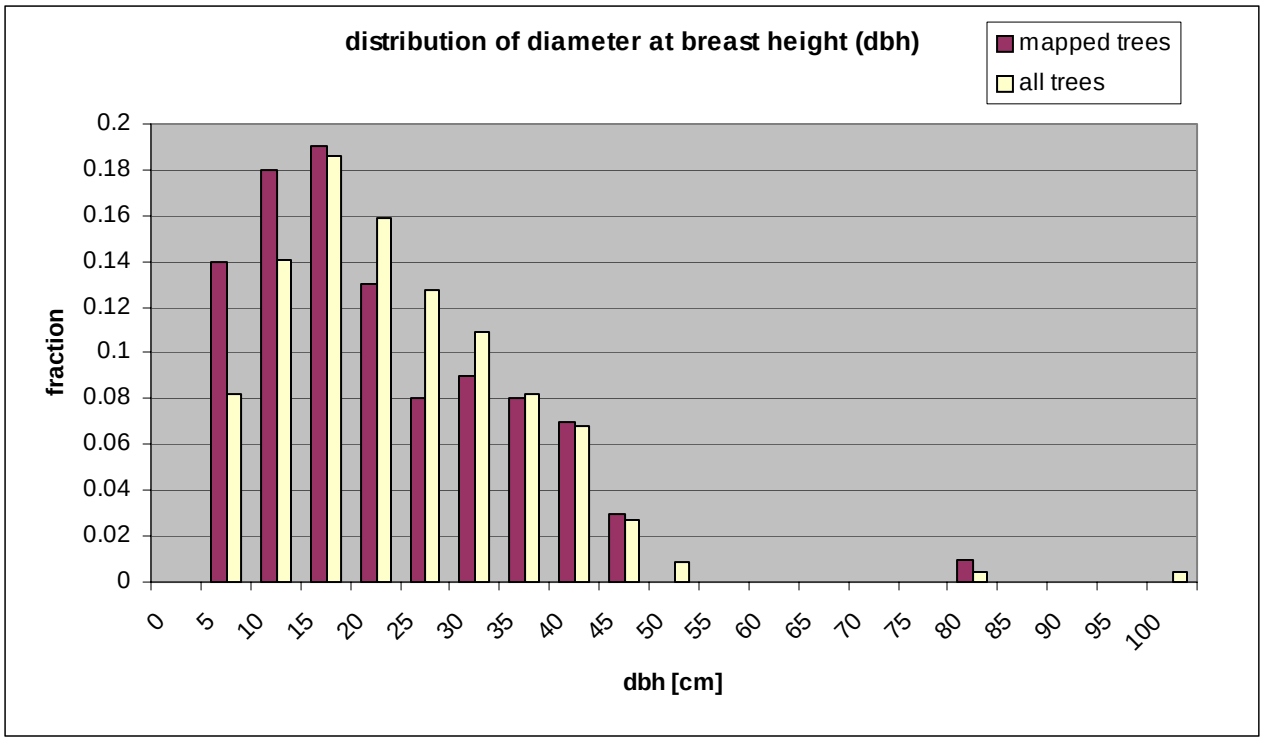

Figure 28 Data of Nancy Kiang

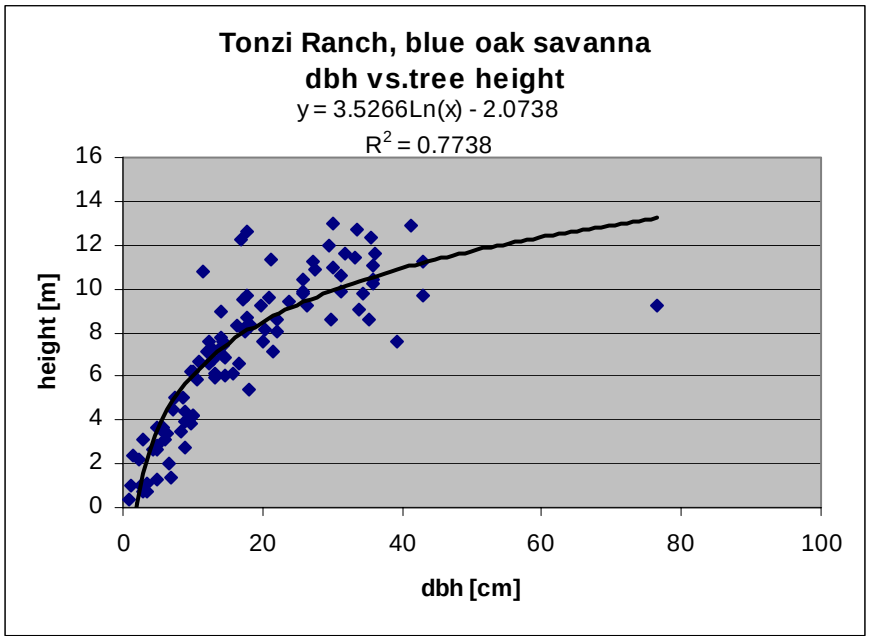

Figure 29 Data of Nancy Kiang

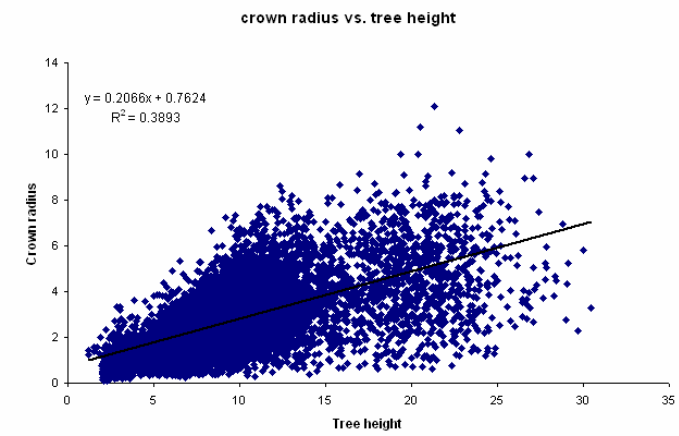

Figure 30 Qi Chen Analyst, LIDAR data

Figure 4. The relationship between crown radius and tree height.

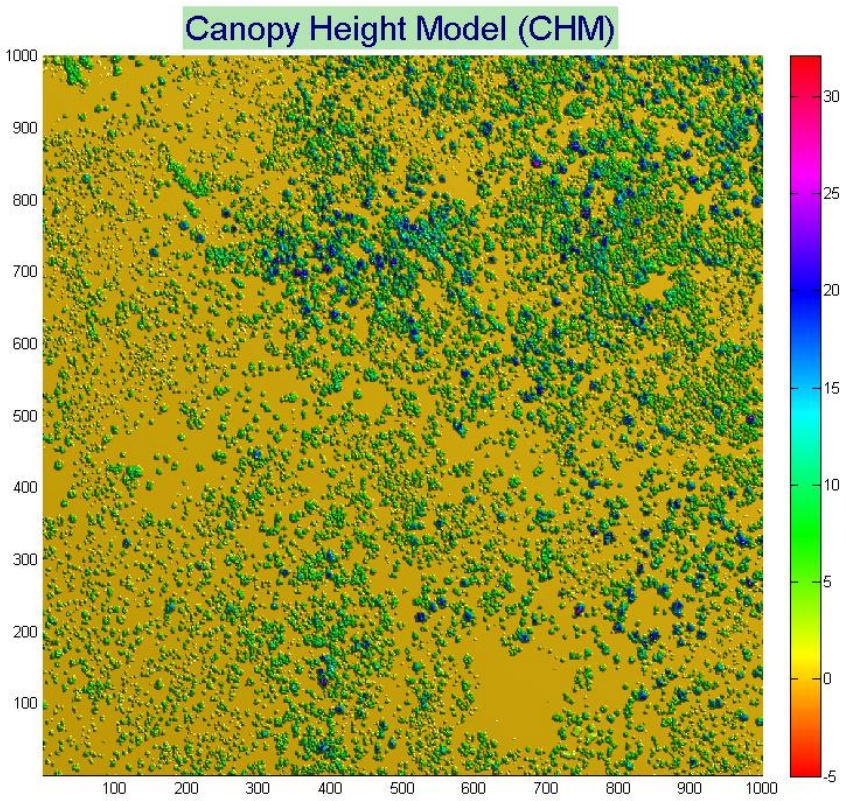

Figure 31 Analysis by Qi Chen

Over the season measurements of leaf area index of the grass and trees were made. The grass LAI was made using destructive sampling in the open and under trees. Typically 3 samples were acquired on an area of 25 by 25 cm.

Leaf Area index transects were produced by Nancy Kiang

Jday	DateVal	DateText	T1	T2	T3	Average
54	3/23/2001	3/23/01	0.67	0.24	0.44	0.45
130	5/1/2001	5/10/01*	0.85	0.37	0.75	0.66
143	5/23/2001	5/23/01	0.93	0.33	0.7	0.65
157	6/6/2001	6/6/01	0.93	0.35	0.71	0.66
186	7/5/2001	7/5/01	0.9	0.29	0.69	0.63
201	7/20/2001	7/20/01	0.99	0.4	0.55	0.65
213	8/1/2001	8/01/01	0.9	0.35	0.71	0.65
254	9/11/2001	9/11/01	0.84	0.38	0.62	0.61

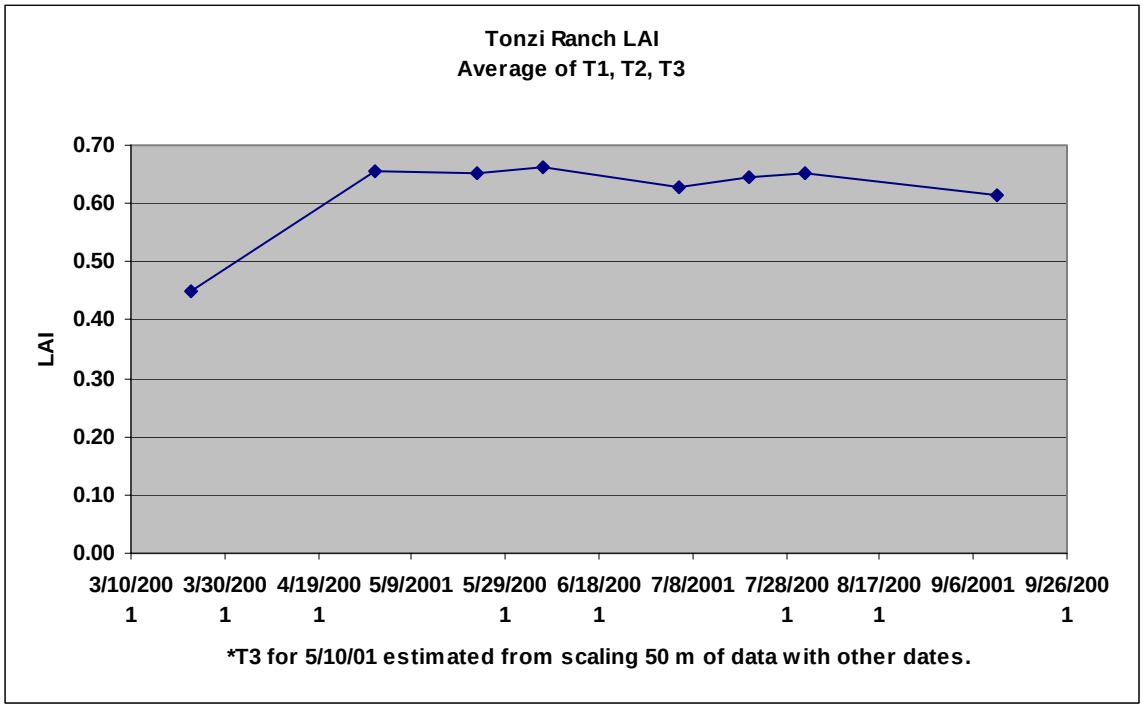

Figure 32 Data of Nancy Kiang

Leaf area index of the trees is being acquired 3 ways. One is via transects and using remote sensing, the LI-2000. The other way is via litter fall. The third way is integration of remote sensing scenes. Each as a different strength, relating to directness of the method and adequacy of spatial averaging. Litterfall is most direct, but most undersampled. The remote sensing is the most indirect, but the method with the best spatial coverage. The transect method falls in between.

Zack Kayler and John Battles

Litter Production of oak trees, for water years (gDM m-2 per year)

02_03: 150.75 (43.35) acorns included
02_03: 115.45 (27.95) no acorns
03_04: 112.70 (12.78)

Photosynthetic Capacity was measured by Liukang Xu during the 2001 growing season on blue oak leaves. A summary of the data follows, and was published in Xu and Baldocchi (2003).

2001 oak leaf Li-Cor6400 data

DOY Vcmax = Rd = Jmax =

18-Apr	108.0000	41.6300	5.0800	89.7400
	108.0000	46.1700	4.7800	61.3200
	108.0000	45.0500	4.0700	119.9400
	108.0000	63.2900	4.1500	143.3000
	108.0000	49.2900	2.7200	123.3000
27-Apr	117.0000	78.7400	1.6800	132.5200
	117.0000	80.8000	1.7800	150.3600
	117.0000	77.8300	1.9900	138.0800
	117.0000	82.9800	1.6900	172.4900
4-May	124.0000	94.1200	1.6480	191.0800
	124.0000	118.2800	2.1510	275.0000
	124.0000	75.7600	1.5330	195.6300
	124.0000	89.4300	1.5850	186.6000
11-May	131.0000	122.0700	0.9900	
	131.0000	106.3900	0.5500	204.2700
	131.0000	97.4300	0.5600	221.6000
17-May	137.0000	127.3000	1.4300	283.9100
	137.0000	112.5000	1.2500	233.3500
	137.0000	113.7500	0.7900	257.8300
24-May	144.0000	103.8400	0.7000	195.8900
	144.0000	92.7800	0.4400	237.9500
31-May	151.0000	84.3400	0.7700	165.0300
	151.0000	94.8800		161.8200
15-Jun	166.0000	99.0000	0.9900	167.3000
	166.0000	60.1100	0.8900	123.8800
	166.0000	70.1000	0.8300	108.8700
28-Jun	179.0000	65.4000	1.0200	106.3800
	179.0000	56.7700	1.0600	103.9400
	179.0000	57.0100	0.7300	89.3100
12-Jul	193.0000	68.8700	0.3200	93.6100
	193.0000	71.1800	0.6200	114.0200
	193.0000	46.4500	0.3300	64.7200
	193.0000	50.5100	0.4000	73.9600

23-Jul	204.0000	60.9000	0.3700	99.2300
	204.0000	46.2700	0.3800	70.9900
	204.0000	43.0200	0.3700	52.1200
30-Jul	211.0000	67.6800	0.5320	81.9700
	211.0000	67.7700	0.2983	84.6400
9-Aug	221.0000	65.1700	0.5300	101.6200
	221.0000	53.1200	0.7200	63.5800
16-Aug	228.0000	56.0000	0.2700	88.0000
	228.0000	32.2400	0.4200	37.1700
	228.0000	13.6300	0.6100	18.1400
23-Aug	235.0000	58.2800	0.6600	72.2000
	235.0000	66.5800	0.4000	85.0000
30-Aug	242.0000	65.1300	0.6450	78.3900
	242.0000	35.6400	0.7920	35.5500
	242.0000	26.2100	0.4900	22.1500
	242.0000	32.6100	0.3170	24.8300
6-Sep	249.0000	20.0900	0.4600	17.6600
	249.0000	38.0900	0.2900	26.6700
	249.0000	35.7600	0.3300	34.0300
13-Sep	256.0000	45.0500	0.4450	47.5300
	256.0000	28.4500	0.6980	27.9100
	256.0000	30.7100	0.5190	29.3000

- 8.1) Table Definition With Comments.

'30 min data for AmeriFlux Web Page

File names:

These data are subject to several data filters. Filtout searches for outliers and replaces them with 9999. These periods are associated with rain events for the most part. Outliers are defined by limits set for variables according to variance, skewness and kurtosis thresholds. They differ for the sonic anemometer and infrared spectrometer. Filtturb is a filter that screens the data for limits according to Monin Obukov scaling theory. Mostly it looks for limits on the standard deviation of w. FiltCO2 screens the CO2 flux data for physiological limits.

Data variables in tower0001dat files

```
/* Headers for output files */

        daytime_," DAYTIME");
        nee_, " NEE umol m-2 s-1");
        fcwpl2d_," FC_WPL_2D umol m-2 s-1");
        wc2d_," WC_2D umol m-2 s-1");
        wc1d_, " WC_1D umol m-2 s-1");
        fc1d_," FC_WPL_1D umol m-2 s-1");
        fcadd_," CO2_Storage umol m-2 s-1");
        co2ppm_, " CO2 LI7500 ppm");
        rhoc_, " RHOC mmol m-3");
        cvolt_, " C volt");
        cc_, " CO2 var");
        skc_, " skewness CO2");
        krc_, " kurtosis CO2");

        rnet_, " Rnet Net Radiation W m-2");
        solar_, " Solar Radiation W m-2");
        parup_, " incoming PAR umol m-2 s-1");
        pardown_, " Par reflected umol m-2 s-1");
        paralbedo_, " PAR albedo ");

        wnddir_," Wind Direction degrees");
        wndspd_, " Wind Velocity m s-1");
        ustar_," Friction Velocity m s-1");
        w_," wbar m s-1");
        ww_," w var");
        angw_, " ang of w rotation");
        sigw_ustar_, " std dev w/ u* ");
        krw_, " kurtosis w");
        zoverl_," z over L");

        leflx_," LE Latent Heat Flux  W m-2");
        rhoq_, " RHOQ mmol m-3");
        qvolt_, " q volt");
        qq_, " q var");
        skq_, " skewness q");
        krq_, "  kurtosis q");

        hflx_," H Sensible Heat Flux W m-2");
        tsonic_, " Tsonic");
        ttsonic_, " T sonic var");
        skt_, "skewness Tsonic");
        krtsonic_, " kurtosis Tsonic");

        parfl_," PAR floor umol m-2 s-1");
        tair_," Tair  C");
        rhov_," absolute humidity  mol m-3");
        vpd_," Vapor pressure deficit  kPa");
        presskpa_," Pressure  kPa");
        precip_," precipitation mm");
        wetness_," wetness ");

        TS2_, "TSOIL2 C");
```

```
        TS4_, "  TSOIL4 C");
        TS8_, " TSOIL8 C");
        TS16_," TSOIL16 C");
        TS32_, " TSOIL32 C");
        gsoil_, " G Soil Heat Flux: W m-2");
        soilmoisturesfc_," soil moisture @ sfc %");
        soilmoisture10_," soil moisture @ 10 cm %");
        soilmoisture20_," soil moisture @ 20 cm %");

        battery_volts," battery volts");
        scan_," Number of scans");
```

9.0) DATA MANIPULATIONS

- 9.1) Formulas.

Subroutine that computes covariances and applies gas law corrections

```
   static void process_flux()
{
float lambda, lfusion, rhoadry, rhomoist, tk, tksonic, cpair, rhovkg, spechum, sig;
float wbarwpl, e_wpl_2d, e_wpl_1d, le1d, ewpl;
float hflx1d, wtguess, wtguess_1d;
float wqq, wqq1d, wtcorr1d, wtcorr2d;
float term1, term2, terma, termb, sig16;
float w_rhov_g_2d, w_rhov_g_1d, rhov_g;
float rhoc_mg_m3;


        wtcorr2d=0;
        wtguess=0;

        wtcorr1d=0;
        wtguess_1d=0;

        tk=out.tair+273.15;
        tksonic=out.tsonic+273.15;

         if(fabs(out.tair)>50)
        {
        tk=tksonic;
        out.tair=out.tsonic;
        }


/*  latent heat of evaporation and fusion */

        lambda = 3149000 - 2370 * tk;  /* MJ kg-1 */
        lfusion = 334000. ;

        if (tk < 273)
```

```
        lambda += lfusion;

        lambda /= 1000.;      /* J g-1  */


/* density of dry air  */

        rhoadry = (out.presskpa - out.ea) * 28.964 / (8.314 * tk); /* kg m-3  */

/* density of moist air */

        rhomoist = (out.presskpa * 28.964 / (8.314 * tk)) * (1. - .378 * out.ea /
out.presskpa);  /* kg m-3 */


/* Weight Cpair according to moist and dry air densities */

        rhovkg=out.rhov*18.0/1000.;  /* absolute moisture denisty, kg m-3, converted
from mol m-3 */

        cpair = 1010. * rhoadry + 4182. * rhovkg;  /* specific heat of moist air */

        spechum = rhovkg / rhomoist;               /* specific humidity, relative to
moist air, kg/kg */

        sig = rhovkg / rhoadry;                    /* specific humidity relative to
dry air, kg/kg */

/*
        Compute WPL corrected sensible heat and latent heat flux densities:

        correct virtual temperature heat flux from sonic to actual heat flux. It is
a function of the specific
        moisture flux density, which in turn is a function of the sensible heat
flux. Since neither is known
        a priori we must iterate.

*/


        do
        {
            wtguess=wtcorr2d;
            wtguess_1d=wtcorr1d;

/*

        Webb et al correction for evaporation flux density

        Ewpl = w'rhov' (1 + (rhov/rhoa)(ma/mv)) + rhov w'T'/T   (g m-2 s-1)

        Make sure the units are correct. The WPL correction was derived from the gas
law:

        rhoa/ma + rhov/mv = P/RT, where rhoa and rhov have units of mass/m3
```

```
*/

        rhov_g=rhovkg*1000.;    /* absolute density of water vapor, g m-3 */

/* convert molar flux density to mass flux density to apply WPL correction to
evaporative flux densities */

        w_rhov_g_2d=out.w_rhov_2d*18./1000.;     /* g m-2 s-1, evaporative flux
density, 2 d rotation */
        w_rhov_g_1d=out.w_rhov_1d*18./1000.;    /* g m-2 s-1, evaporative flux
density, 1 d rotation */

        e_wpl_2d = (1. + sig * 1.607) * w_rhov_g_2d + rhov_g * wtguess / tk;  /* g
m-2 s-1 */

        e_wpl_1d = (1. + sig * 1.607) * w_rhov_g_1d + rhov_g * wtguess_1d / tk; /* g
m-2 s-1  */

/*

divide factor of 1000 is needed to change e_wpl from g m2 s-1 to kg m-2 s-1,
so units cancel when divided by rhoa_moist (kg m-3)

*/

        wqq = e_wpl_2d * (1. - spechum) / (1000. * (rhomoist));  /* m s-1  */

        wqq1d = e_wpl_1d * (1. - spechum) / (1000. * (rhomoist));  /* m s-1 */

/*
Correct the sonic virtual heat flux and convert it to a true
thermodynamic sensible heat flux covariance, as adjusted for
moisture flux

*/
        wtcorr2d = (out.wt2d - .51 * tk * wqq) / (1. + .51 * spechum) ;       /* K m
s-1  */

        wtcorr1d = (out.wt1d - .51 * tk * wqq1d)/ (1. + .51 * spechum) ;    /* K m
s-1 */

        }while(fabs((wtcorr2d-wtguess)/wtcorr2d) > 0.01);


/* Sensible heat flux with 2-D rotation */

        out.hflx = wtcorr2d * cpair;    /* W m-2  */


/* Sensible heat flux with 1-D rotation  */

        hflx1d = wtcorr1d * cpair;    /* W m-2 */

/* Latent heat flux with 2-D rotation */

        out.leflx = lambda * e_wpl_2d;  /* W m-2  */
```

```
/* Latent heat flux with 1-D rotation  */

        le1d = lambda * e_wpl_1d;       /* W m-2 */

        if (in.wx2d[3] == 9999)
        {
        wtcorr2d = 9999;
        wtcorr1d = 9999;
        out.hflx = 9999;
        }

        if (in.wx2d[4] == 9999)
        {
        e_wpl_2d = 9999;
        e_wpl_1d = 9999;
        wqq = 9999;
        wqq1d = 9999;
        out.leflx=9999;
        le1d = 9999;
        ewpl = 9999;
        e_wpl_1d = 9999;
        w_rhov_g_2d=9999;
        }

/*

CO2 fluxes, Webb et al. density corrections

The new Licor LI-7500 measures mole density. I need to convert to mass density, then
apply wpl corrections

*/


        out.co2ppm=out.rhoc*28.96/rhoadry;       /* CO2 conc ppm */

        sig16 = sig * 1.6077;                       /* (ma/mv)(rhov/rhoa) */

        wbarwpl = 1.6077 * w_rhov_g_2d / (1000.* rhoadry) + (1. + sig16) * wtcorr2d
/ tk;  /* m s-1 */

        rhoc_mg_m3=out.rhoc*44.;                   /* convert mol density of CO2 to
mass density */

        term1 = 1.6077 * w_rhov_g_2d * rhoc_mg_m3 / (1000.* rhoadry);  /* mg CO2  m-
2 s-1 */

        terma = 1.6077 * w_rhov_g_1d * rhoc_mg_m3 / (1000. * rhoadry);  /* mg CO2 m-
2 s-1 */

        term2 = (1. + sig16) * rhoc_mg_m3 * wtcorr2d / tk;     /* mg CO2 m-2 s-1 */

        termb = (1. + sig16) * rhoc_mg_m3 * wtcorr1d / tk;   /* mg CO2 m-2 s-1 */
```

```
        if (wtcorr2d == 9999)
        term1 = 9999;

        if(w_rhov_g_2d == 9999)
        term2 = 9999;

        /* WPL Correction */

        if((term1 != 9999) && (term2 != 9999) && (out.wc2d != 9999))
        {

        /* 2d CO2 Flux */
        out.fc_wpl_2d = out.wc2d + 1000. * (term1 + term2)/44.;   /* micromol m-2 s-
1 */

        /* 1d CO2 flux */
        out.fc_wpl_1d = out.wc1d + 1000. * (terma + termb)/44.;   /* micromol m-2 s-
1 */
        }
        else
        {
        out.fc_wpl_2d = 9999;
        out.fc_wpl_1d = 9999;
        }

        if (in.wx2d[5]==9999)
        {
        out.fc_wpl_2d = 9999;
        out.fc_wpl_1d = 9999;
        }

return;
/* end of process flux */
}
```

Campbell Data Logger Programs

CR23x3

Soil Moisture Forest Floor

Inputs

```
;:panel_t
;:bat_v
;:SoilM_1
;:SoilM_2
;:SoilM_3
;:SoilM_4
;:SoilM_5
;:SoilM_6
```

```
;:SoilM_7
;:q_line
;:NR_1
;:NR_2
;122 Output_Table  30.00 Min
;1 122 L
;2 Day_RTM  L
;3 Hour_Minute_RTM  L
;4 panel_t_AVG  L
;5 bat_v_AVG  L
;6 SoilM_1_AVG  L
;7 SoilM_2_AVG  L
;8 SoilM_3_AVG  L
;9 SoilM_4_AVG  L
;10 SoilM_5_AVG  L
;11 SoilM_6_AVG  L
;12 SoilM_7_AVG  L
;13 q_line_AVG  L
;14 NR_1_AVG  L
;15 NR_2_AVG  L
```

Met on Tower

```
CR23X6

Input Table

;:Panel_T
;:Batt_Volt
;:Pricip_mm
;:Par_up
;:Par_Dn
;:Par_Calib
;:Pyranom
;:Net_Rad
;:Temp_Amb
;:RH
;:L_PAR1
;:L_PAR2

;131 Output_Table  30.00 Min
;1 131 L
;2 Day_RTM  L
;3 Hour_Minute_RTM  L
;4 Panel_T_AVG  L
;5 Batt_Volt_AVG  L
;6 Pricip_mm_TOT  L
;7 Par_up_AVG  L
;8 Par_Dn_AVG  L
;9 Par_Calib_AVG  L
;10 Pyranom_AVG  L
;11 Net_Rad_AVG  L
;12 Temp_Amb_AVG  L
;13 RH_AVG  L
;14 Par_up_STD  L
```

```
;15 Par_Dn_STD  L
;16 Par_Calib_STD  L
;17 Pyranom_STD  L
;18 Net_Rad_STD  L
;19 Temp_Amb_STD  L
;20 RH_STD  L
;
```

The new wind speed profile system has been installed on 5 levels. The data logger program was written for 6 levels.
The lowest level is labeled 1 and the highest is labeled 6.

Output is as follows:
Final Storage Label File for: WSP1.CSI
Date: 8/1/2003
Time: 12:09:19

105 Output_Table 30.00 Min
1 105 L
2 Day_RTM H
3 Hour_Minute_RTM H
4 Panel_T_AVG H
5 Batt_V_AVG H
6 WS_1_AVG H
7 WS_2_AVG H
8 WS_3_AVG H
9 WS_4_AVG H
10 WS_5_AVG H
11 WS_6_AVG H
12 WD_1_AVG H
13 WD_2_AVG H
14 WD_3_AVG H
15 WD_4_AVG H
16 WD_5_AVG H
17 WD_6_AVG H
18 WS_1_STD H
19 WS_2_STD H
20 WS_3_STD H
21 WS_4_STD H
22 WS_5_STD H
23 WS_6_STD H
24 WD_1_STD H
25 WD_2_STD H
26 WD_3_STD H
27 WD_4_STD H
28 WD_5_STD H
29 WD_6_STD H
30 WS_1_MAX H

31 WS_1_Hr_Min_MAX H
32 WS_2_MAX H
33 WS_2_Hr_Min_MAX H
34 WS_3_MAX H
35 WS_3_Hr_Min_MAX H
36 WS_4_MAX H
37 WS_4_Hr_Min_MAX H
38 WS_5_MAX H
39 WS_5_Hr_Min_MAX H
40 WS_6_MAX H
41 WS_6_Hr_Min_MAX H
42 WD_1_MAX H
43 WD_1_Hr_Min_MAX H
44 WD_2_MAX H
45 WD_2_Hr_Min_MAX H
46 WD_3_MAX H
47 WD_3_Hr_Min_MAX H
48 WD_4_MAX H
49 WD_4_Hr_Min_MAX H
50 WD_5_MAX H
51 WD_5_Hr_Min_MAX H
52 WD_6_MAX H
53 WD_6_Hr_Min_MAX H
54 WS_1_MIN H
55 WS_1_Hr_Min_MIN H
56 WS_2_MIN H
57 WS_2_Hr_Min_MIN H
58 WS_3_MIN H
59 WS_3_Hr_Min_MIN H
60 WS_4_MIN H
61 WS_4_Hr_Min_MIN H
62 WS_5_MIN H
63 WS_5_Hr_Min_MIN H
64 WS_6_MIN H
65 WS_6_Hr_Min_MIN H
66 WD_1_MIN H
67 WD_1_Hr_Min_MIN H
68 WD_2_MIN H
69 WD_2_Hr_Min_MIN H
70 WD_3_MIN H
71 WD_3_Hr_Min_MIN H
72 WD_4_MIN H
73 WD_4_Hr_Min_MIN H
74 WD_5_MIN H
75 WD_5_Hr_Min_MIN H
76 WD_6_MIN H
77 WD_6_Hr_Min_MIN H

- 9.1.1 Derivation Techniques/Algorithms.

none provided.

- 9.2) Data Processing Sequence.

Flux covariances are computed in the field by the data acquisition program. Back at home, calibrations are double and triple checked by comparing old and new calibrations and by comparing the mean response of the scalar flux sensors against independent meteorological instruments. Tests are made for energy balance closure to ensure that the data are of reliable quality. Programs are then run to delete periods when the sensors were off line, off range, being maintained or un-reliable due to rain or instrument malfunction.

- 9.2.1 Processing Steps and Data Sets.

Flux data: all the flux data are organized in the following way

			Typically, each folder has subfolder
Floor_2001	eg.	**Floor_2001**	
Floor_2002			Datalogger Notes
Floor_2003			Floor_C++ code
Floor_2004			flux
Floor_interannual			flux_fromfield
			met
Tower_2001			raw
Tower_2002			sapflow
Tower_2003			Sum_data
Tower_2004			
Tower_interannual		**Vaira_2003**	Datalogger Notes
			flux
Vaira_2000			flux_fromfield
Vaira_2001			met
Vaira_2002			raw
Vaira_2003			Sum_data
Vaira_2004			Vaira03_C code
Vaira_interannual			

In the subfolder, *Datalogger Notes*, you will find two files called,
cr10x_heading 2001_fl.xls
cr23x_heading 2001_fl.xls
They are very important files, containing all the information of outputs from soil and met sensors for each EC system. They also contain the information about when Ted adds new sensors or removes sensors, or rearranges the sequence of output, or changes the output from engineering unit to mv. Sometime I also include the calibration factor, but if not, it should be in the subroutine (*calibration*) of C++ program file.

In the subfolder, *Floor_C++ code*,
It contains two C++ code files,
raw_floor2001.c for raw data processing
and *flux_floor2001.c* for flux computation

Subfolder, *flux*, contains all the output files from the raw_floor2001.c code, including;

*.spk
*.err_dspk
*.flx_dspk
*.nrt_dspk

Subfolder, *flux_fromfield*, contains all the **.NRT, *.FLX, *.ERR* files, they are from field laptop. They are just for diagnostic purpose, you don't need them to compute the EC flux.

Subfolder, *met*, contain all the daily met and soil data.
For examples, *tz2_01DOY.10x* and *tz3_01DOY.23x*

Subfolder, *raw*, contains no file. This folder I used to prepare, rename and clean raw files. After done, I copy all the raw data files to *F:* drive.

Subfolder, *Sum_data*, contains all the sigmaplot files and the output file from *flux_floor2001.c* C++ code; i.e. *Tonzi_understory2001.dat.*

In folders, *Tower_2003 and Tower_2004*, I have two additional subfolders, called *CO2Profile* and *Windprofile*, which contain all the CO2 and wind profiles data.

In folders, *Floor_interannual*, *Tower_interannual*, *Vaira_interannual*, I have some files for the interannual comparison of flux (F_c, *LE*, *H*, and radiation components) for each EC system.

All the EC raw data, processed data, met and soil data have been backuped on H205-3 computer.

In the folder, *LI_COR7500*, it contains all the calibration data for our six licor 7500.

Section two: Process EC flux

Data preparation

a. Met and soil data: Break down to daily files if the laptop is not working around mid-night. Also make sure each met and soil file start with 0030 and end with 2400.

b. Raw data file: currently, the names for all the raw data file generated by gillsonic.exe from three EC systems are as following;

DOY	Vaira	Tower	Floor
1-9	V?time.raw	T?time.raw	F?time.raw
10-99	V??time.raw	T??time.raw	F??time.raw
100-365	V???time.raw	T???time.raw	F???time.raw
* ? represents DOY			
time: 4 digits time			

C++ code can't process the raw data with this kind file names. To have the right file name as I listed in the following table, I create a batch file to rename all the files. How to create the batch file? Please read the email message at your left on the glass door of the cabinet. It is very simple and fast!

After rename

DOY	Vaira	Tower	Floor
1-9	V00?time.raw	T00?time.raw	F00?time.raw

10-99	V0??time.raw	T0??time.raw	F0??time.raw
100-365	V???time.raw	T???time.raw	F???time.raw

Also another minor thing you need to do is to rename all the raw data file *VDOY0000.raw* by add 1 on DOY.

I think these file naming problems can be fixed by modifying the source code of gillsonic.exe.

If more than one raw data file in 0.5 hr, I delete one. This could happen at 4:30am when watchdog program reboots the EC systems, or when we are out there to download the data.

I do all these raw data preparation on folders on C: Drive, then copy to appropriated folder on F: Drive.

Last thing is to run *raw_floor2004.exe* and *flux_floor2004.exe* C++ code to compute the flux.

Plot the flux using sigma-plot, check all the flux data (F_c, *LE*, *H*, and *G*), CO_2 and water vapor concentrations, met and soil data, make sure they are all in the right ranges. If any data you think it is not right, talk to Dennis or Ted.

10.0) ERRORS

- 10.1) Sources of Error.

- 10.2) Quality Assessment.

Surface energy balance is tested by comparing measurements of available energy against the sum of latent and sensible heat flux.

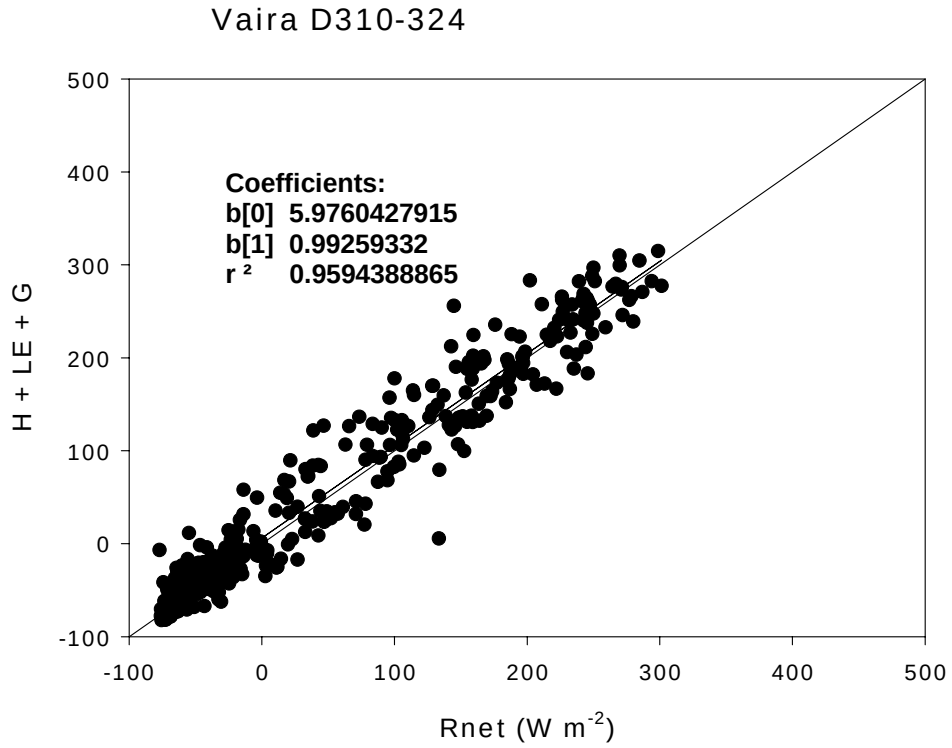

- 10.2.1) Data Validation by Source.

- 10.2.2 Confidence Level/Accuracy Judgement.

The following are the best estimates of accuracy for a single flux estimate:

Net radiation +/- 4 to 7%
Soil heat flux +/- 10%
Latent heat flux +/- 15 to 20 % or +/-30 W m^2, which ever is larger
Sensible heat flux +/- 15 to 20 % or +/-30 W m^2, which ever is larger
None of these estimates addresses the variability of flux estimates from site to site.

Detection limit of CO2 flux system: 0.025 mg m-2 s-1

The intermittency of turbulence limits the sampling error of turbulent fluxes to 10 to 20%. On top of this we have to deal with measurement errors. Fortunately, lots of statistically averaging reveals stable fluxes and small bias errors (< 12%) on the surface energy fluxes.

- 10.2.3 Measurement Error for Parameters and Variables.

11.0) NOTES

11.1) Known Problems With The Data.

As the duration of the experiment has continued we are finding that soil heat flux is biased low at the Vaira and Tonzi ranches. The soil heat flux plates are in cow proof enclosures, so insulating biomass is accumulating over the sensors and is insulating them. Plus grass is taller in the cow proof areas, so less energy reaches the ground. We have seen energy balance closure degrade from near 95% at the beginning of the Vaira study to about 75% circa 2003.

The radiation boom from the tower was initially only a meter away. Plus the tower was put in the open, so the values of albedo and net radiation may be biased. In the spring of 2004 we extended the radiation boom out about 3 m to give the sensors a better view of the soil system.

11.2) Usage Guidance.

12.0) REFERENCES

Publications Generated From this Project

Baldocchi, D.D., Xu, L. and Kiang, N., 2004. How plant functional-type, weather, seasonal drought, and soil physical properties alter water and energy fluxes of an oak-grass savanna and an annual grassland. Agricultural and Forest Meteorology, 123(1-2): 13-39.

Tang J, Baldocchi D D., Qi Y, Xu L. 2003. Assessing soil CO_2 efflux using continuous measurements of CO_2 within the soil profile with small solid-state sensors. *Agricultural and Forest Meteorology* (submitted, Dec. 2002; Accepted March, 2003).

Xu L, Baldocchi DD. 2003. Seasonal trend of photosynthetic parameters and stomatal conductance of blue oak (*Quercus douglasii*) under prolonged summer drought and high temperature *Tree Physiology* 23, 865-877.

Xu, L. and Baldocchi, D.D., 2004. Seasonal variation in carbon dioxide exchange over a Mediterranean annual grassland in California. Agricultural and Forest Meteorology, 123(1-2): 79-96.

Baldocchi, D.D., Tang, J. and Xu, L., 2006. How Switches and Lags in Biophysical Regulators Affect Spatio-Temporal Variation of Soil Respiration in an Oak-Grass Savanna. Journal Geophysical Research, Biogeosciences, 111: G02008, doi:10.1029/2005JG000063.

Baldocchi, D. and Xu, L., 2005. Carbon excahnge of deciduous broadleaved forests in temperature and Mediterranean regions. In: H. Griffiths and P. Jarvis (Editors), The Carbon Balance of forest biomes. Taylor and Francis, Andover, Hampshire, United Kingdom, pp. 187-216.

Baldocchi, D.D. et al., 2005. Predicting the onset of net carbon uptake by deciduous forests with soil temperature and climate data: a synthesis of FLUXNET data. International Journal of Biometeorology, 49(DOI: 10.1007/s00484-005-0256-4): 377-387.

Acknowledgements

Ranch Owner:
Mr Russell Tonzi
Ione Ca

Field Assistance:
Liukang Xu, Ted Hehn, Nancy Kiang, Lianhong Gu, Jianwu Tang, Kevin Tu, Francesca Ponti, Laurent Misson, John Battles, Randy Jackson.

Funding

US Dept of Energy, Terrestrial Carbon Program, Roger Dahlman administrator
California Agricultural Experiment Station
Kearney Soil Science Foundation, Kate Scow
WESTGEC, NIGEC, Susan Ustin adminsitrator

Contribution to
AmeriFlux and Fluxnet programs